Flip-Chip Fabry-Perot Electron Interferometer

Samuel Gaucher

Department of Physics
McGill University
Montréal, Québec, Canada
December 2015

A thesis submitted to McGill University
in partial fulfillment of the requirements of the degree of
Master of Science.

Acknowledgments

First and foremost, I wish to thank Prof. Guillaume Gervais, supervisor, leader and captain of the Gervais crew. Your contagious dynamism, enthusiasm and strong spirit were sources of daily motivation. Thank you for your protective support, firm confidence, and indulgent cuisine.

This entire research would not have been possible without the original flip-chip idea formulated and developed by Ph.D. Keyan Bennaceur, before my arrival and throughout my time in the lab. Thank you for your guidance along my participation to your original project, and for helping me bring my contributions to reality. I am grateful for the innumerable hours you spent with me, whether in the cleanroom teaching me the rudiments of nanofabrication, or in the lab explaining the how-tos of low-temperature physics. For all that I have learned from you, I cannot express enough recognition.

Wholeheartedly, I wish to thank the computer pros of the lab, Ben Schmidt and Pierre-Franņis Duc. I can not overlook your major contribution to my education as a scientist. Your knowledge was of prime importance, and I could not have found more resourceful persons. Thanks as well to all other members of the Gervais lab, Matei Petrescu, Dominique Laroche, Simon Bilodeau, Alex Vlasov, Olivier Cyr-Choinière and Nicolas Doiron-Leyrand, for your support and help.

Finally, special recognition goes to the technicians Robert Gagnon, John Smeros and Richard Talbot for their devoted and precious assistance. Thanks as well to the staff members of the McGill Nanotools Microfab, Lino Eugene, Don Berry, John Li, Sasa Ristic and Matthieu Nannini. Without your help, samples and experiments would not see the light of day, and doing science would be much harder.

Abstract

The fractional quantum Hall effect (FQHE) is well understood in within the composite fermions picture: in 2+1 dimensions, a change in the topology of electron configuration space leads to the emergence of *anyons*, quasiparticles with fractional exchange statistics ranging between Bose-Einstein and Fermi-Dirac. These composite fermions, made of electrons bound to magnetic flux quanta in a ratio expressed by the filling factor ν, act as charge carriers in two-dimensional electron gases (2DEG) and give rise to exotic Hall magnetoresistance quantization. However, the elusive $\nu = 5/2$ state of the FQHE seems to contain additional structure from which an even more peculiar behavior could arise. The excitations of this state are speculated to display non-abelian braiding statistics, an aspect which raised significant interest due to possible Majorana-like quantum computing applications.

In order to probe the statistics of the 5/2 state and verify if it has a non-abelian nature, it has been suggested to conduct interferometry experiments in which quasiparticles are undergoing braiding operations. Such experiments have been used in other states of the FQHE, confirming the existence of anyons and fractional statistics. Despite sustained effort, it has not yet been possible to achieve convincing interference measurements in the 5/2. The difficulty of this task is explained by the extreme fragility of the state, which appears only in pure ultra-high mobility 2DEG samples. It is believed, in addition, that the nanofabrication of interferometers on these substrates can induce impurities, notably through e-beam lithography, making it difficult to observe strong 5/2 features.

To tackle the fragility of the 5/2 state, this research proposed to implement a *flip-chip* Fabry-Perot interferometer. The idea behind the flip-chip method is to fabricate the interferometers on separate substrates and to flip them on the 2DEG samples, as if they had originally been patterned on them. This approach leaves the 2DEG in pristine condition, hopefully increasing the chances of conducting convincing interferometry experiments. At this point, it has been possible to demonstrate that the flip-chip method works for low-dimensional transport experiments. Quantum point contacts (QPCs) mounted in flip-chip configuration could reproduce the characteristic 2DEG conductance pinch-off and quantization ($2e^2/h$). Interferometers could be unmounted and retested on different 2DEGs, maximizing the nanofabrication yield. Signs of what could possibly be quantum interference of electrons have also been observed, although not on 2DEGs of high enough mobility to study the 5/2 state.

Abrégé

L'effet Hall quantique fractionnaire (EHQF) est aujourd'hui bien compris dans le cadre du modèle des fermions composites: en 2+1 dimensions, la topologie de l'espace de configuration des électrons change et entraîne l'émergence de ce que l'on nomme des *anyons*, des quasiparticules dont l'interversion est décrite par des statistiques fractionnaires à mi-chemin entre les statistiques de Bose-Einstein et Fermi-Dirac. Ces fermions composites, faits d'électrons attachés à un certain nombre de quanta de flux magnétique dans un ratio ν, agissent à titre de porteur de charge dans les gaz d'électrons bidimensionnels (2DEG) et donnent lieu à une quantification exotique de la magnétorésistance de Hall. Néanmoins, l'énigmatique état $\nu = 5/2$ de l'EHQF semble détenir une structure additionnelle, de laquelle surgirait une propriété encore plus particulière. Il est spéculé que les quasiparticules de l'état 5/2 soient régies par des statistiques d'échange non-abéliennes, un aspect qui a soulevé l'attention en raison de la possibilité d'effectuer des opérations de calcul quantique au même titre qu'avec les particules théoriques de Majorana.

Dans le but d'étudier les statistiques d'échange de l'état 5/2 et de vérifier si celles-ci sont de nature non-abélienne, il a été suggéré d'entreprendre des expériences d'interférométrie au cours desquelles les quasiparticules sont soumises à des opérations de tressage. De telles expériences ont été réalisées dans d'autres états de l'EHQF, et ont confirmé l'existence des anyons et statistiques fractionnaires. En dépit d'efforts soutenus, il n'a toujours pas été possible d'effectuer des mesures d'interférométrie dans l'état 5/2 de manière convaincante. La difficulté de cette tâche s'explique par l'extrême fragilité de l'état, qui ne se manifeste que dans les échantillons 2DEG de grande pureté et mobilité. De plus, nous croyons que certaines étapes impliquées dans la nanofabrication d'interféromètres, notamment la lithographie à faisceau d'électrons, introduit des impuretés qui rendent difficile l'observation de l'état 5/2.

Pour surmonter cette difficulté, ce projet de recherche propose de mettre en place des interféromètres de Fabry-Pérot en utilisant une configuration de *puce retournée*. L'idée derrière la puce retournée est de fabriquer des interféromètres sur un substrat à part, et de les retourner sur la surface des échantillons 2DEG comme s'ils avaient été créés sur ceux-ci à l'origine. Cette approche offre l'avantage de laisser les échantillons 2DEG dans une condition impeccable, ce qui, nous l'espérons, augmente les changes de pouvoir observer des interférences quantiques. À ce jour, il a été possible de démontrer que la méthode de la puce retournée fonctionne pour réaliser des expériences de trans-

port électronique à basse dimension. Un point de contact quantique (QPC) retournée a pu reproduire avec succès les caractéristiques pincement et quantification ($2e^2/h$) de la conductance d'un 2DEG. Certains interféromètres ont pu être démontés et testés de nouveau sur différents échantillons, maximisant ainsi le taux de succès de la nanofabrication. De plus, des indices de ce qui pourrait s'avérer être des interférences d'électrons ont été observés, quoique ceux-ci se manifestent dans des échantillons 2DEG de qualité inférieure qui ne permettent pas l'étude de l'état 5/2.

Contribution

My contribution to this project has been mainly centered on the fabrication and preliminary tests of the devices. The original flip-chip idea was proposed by Prof. G. Gervais and K. Bennaceur (Ph.D.), who remained in charge of the project. The published measurements [1] were acquired collaboratively between Ph.D. candidate B. A. Schmidt and K. Bennaceur.

The flip-chip interferometer project proposes to implement a novel way to do low-dimensional transport experiments. The abundant nanofabrication challenges required significant effort before interferometry measurements could take place. Together with K. Bennaceur, I was involved in most of the nanofabrication steps: cleanroom processes, e-beam lithography, interferometer design, metal deposition and lift-off, cleaning, flip-chip assembly, soldering. I then tested the devices in order to determine whether some of the features that are essential to achieve anyon interference were present or not. This usually meant performing low-noise measurements at cryogenic temperatures, measuring contact resistance and (quantized) conductance across quantum point contacts.

Contents

Chapter 1

Introduction

1.1 Experimental context

The fractional quantum Hall effect (FQHE) is a fertile research ground to observe a number of phenomena that arise from topological principles: in two dimensions, fermions can behave in a quite unconventional and novel way, as the topology of their configuration space plays a major role on the nature of their exchange statistics. The FQHE involves *anyons* [2], quasiparticles carrying fractional charges and obeying fractional statistics (ranging between bosonic and fermionic statistics). By now, the role of anyons in the FQHE is well understood within the composite fermions model [3]. However, this model only allows for *odd* denominator filling fractions. Since its first observation in 1987 by Willett *et al.* [4], the $\nu = 5/2$ state of the FQHE stood up as the exception to this rule, and has remained one of the most persistent problems in condensed matter physics.

Among the theoretical models proposed to explained the 5/2 state, the Moore-Read Pfaffian [5] attracted considerable attention. The model predicts that the excitations of the state contain additional structure from which an even more exotic behavior could emerge. In fact, the 5/2 quasiparticles should not only obey anyonic statistics, but *non-abelian* exchange statistics. A. Y. Kitaev later suggested [6], in addition, that it would be possible to take advantage of the non-abelian nature of the state to build a fault-tolerant topologically protected quantum computer. Briefly, excitations obeying non-abelian statistics refers to the fact that an exchange of identical particles would not result in a statistical phase factor, but in a completely *different* state. The quasiparticles found in the 5/2 state are for that reason referred to as anyonic Majorana bound states [7]. Observing such particles would be a great discovery in itself, irregardless of the possible quantum computing applications.

In order to probe the statistics of the 5/2 state, many suggested to proceed through anyon interferometry [8–12]. Such experiments have been realized in other states of the FQHE, demonstrating the existence of fractional statistics [13–16]. Investigations of that nature have also be undertaken in the 5/2 state [17, 18], however the outcome is insufficient to confirm or infirm the non-abelian nature of the quasiparticles found in this FQH state. The main problem is that the 5/2 state is extremely fragile, and appears only in the highest purity two-dimensional electron gas (2DEG) samples. Also, it is believed that the processes involved in the fabrication of anyon interferometers, notably e-beam lithography, can introduce impurities that will tarnish irreparably the quality of the 2DEGs, making it impossible to observe strong 5/2 features.

In response to this problem, this research proposes to tackle the fragility of the 5/2 state by implementing a *flip-chip* electron (and eventually anyon) interferometer in order to probe the statistics of the quasiparticles it contains. The idea behind the flip-chip method is to create the interferometer on a separate substrate, and to flip it on the surface of a 2DEG sample as if it had initially be created on it. By doing so, the damaging processes are carried out on less delicate substrates, leaving the 2DEGs as pristine as possible. The results of our flip-chip method were presented recently [1]. Other groups have also been working on similar techniques, confirming that electron interference can be observed using flip-chip Fabry-Perot geometries [19].

1.1.1 Outline

In the first chapter, the basics of low-dimensional physics will first be presented in order to give an idea of the importance of topology in condensed matter physics. With the concept of anyon in mind, the theory behind the FQHE will be exposed, starting from the classical Hall effect. Interferometry experiments will then be explained, with a focus on how a non-abelian signature could be detected. In the second chapter, the fundamental novelty of the flip-chip method will be presented. The third chapter will then be a technical description of the fabrication and testing of the flip-chip interferometers. Finally, chapter four will discuss the results obtained and the actual status of the flip-chip method, and then address the main issues encountered.

1.2 Low-dimensional physics

Low-dimensional physics constitute an active field of research in condensed matter physics. It is therefore important to understand how making experiments in lower dimensions is possible, and what happens to the physics of such systems. One of the reasons behind the interest for lower dimensions is rooted in highly mathematical concepts (whose details are beyond the scope of this research). In short, the heart of the problem lies in the fundamental importance of topology when comes time to understand certain aspects of quantum mechanics. As one reduces the number of spacial dimensions, the notion of indistinguishability of identical particles must be rethought. This has consequences on quantum statistics, hence on how elementary particles are categorized. Concurrently, the interaction effects between spatially confined particles become more important, which enables the emergence of new many-body phenomena.

1.2.1 Topology and statistics

In quantum mechanics, three-dimensionality of space is at the heart of the spin-statistics theorem. In three (or higher) space dimensions, all particles must either have spin $n\hbar$ or $(2n+1)\hbar/2$ with $n = 0, 1, 2...$, known respectively as bosons or fermions [20]. The spin-statistics theorem relates the spin of these particles to their quantum statistics: bosons obey Bose-Einstein statistics and fermions obey Fermi-Dirac statistics, meaning that the wavefunction of a system of identical bosons remains unchanged upon exchange of two particles, while the wavefunction of a system of identical fermions changes sign upon exchange of two particles.

In the context of quantum mechanics, the term *exchange* is rather delicate to use.

One should only remember that quantum statistics refer to the *phase* picked up by the wavefunctions (0, ± 1) upon an *adiabatic* transport of particles which really creates an exchange. This precaution ensures that we treat the exchange not only as a swap of the particles coordinates, but rather as a path dependent process which effectively relates the particle statistics to the topology of the configuration space.

The possible phase factors acquired by the wavefunction along different interchange paths must define a representation of the first homotopy group of the configuration space [20]. In three dimensions, the configuration space is a doubly connected sphere, whose first homotopy group is the *permutation* group S_N. The permutation group has only two one-dimensional representations: identical and alternating, corresponding to Bose-Einstein and Fermi-Dirac statistics [20]. In short, three-dimensional space imposes wavefunctions to describe particles as either being bosons or fermions.

1.2.2 Anyons and fractional statistics

In two dimensions, the topology of the configuration space changes, and one must rethink how the exchange of identical particles operates. This has drastic consequences on the statistics of the confined particles: while only bosons and fermions can exist in three dimensions, two-dimensional particles are not restricted to these categories. In fact, one finds that the first homotopy group of the two-dimensional configuration space is the *braid* group B_N, which admits a continuous range of one-dimensional representations [20]. In other words, the phase factor picked up by a wavefunction upon exchange of those particles can range continuously from -1 to 1, giving rise to statistics in-between Bose-Einstein and Fermi-Dirac. Wilczek coined the term *anyons* in 1982 [2] to describe these two-dimensional particles obeying "any" statistics, or *fractional* statistics.

For a two-particle wavefunction $|\psi_1\psi_2\rangle$, a three-dimensional exchange yields a plus or minus sign

$$|\psi_1\psi_2\rangle = \pm\,|\psi_2\psi_1\rangle \tag{1.1}$$

such that the wavefunction is symmetric for bosons and antisymmetric for fermions.

The two-dimensional anyonic exchange relation is represented by

$$|\psi_1\psi_2\rangle = e^{i\theta}\,|\psi_2\psi_1\rangle \tag{1.2}$$

with phase angle θ between 0 and π. As a result, three-dimensional exchange operations become, in two dimensions, topologically protected *braiding* operations which are 'impossible to untangle'.

The most prominent realization of anyons is in the fractional quantum Hall effect [20–22], which will be explained in details later. For now, it suffices to say that the effect is due to quasiparticles —composite fermions— existing only in two dimensions, composed of electrons bound to magnetic flux quanta (vortices) in a ratio represented by the filling factor ν. Those composite fermions fit the requirements for being anyons [21], with fractional phase angle given by

$$\theta = \nu\pi. \tag{1.3}$$

1.2.3 Two-dimensional systems

One could express doubts about the physical meaning of lower spacial dimensions beyond sole theoretical speculation. Indeed, the mathematical language is rich enough to describe a space of arbitrary dimensions. It is therefore possible to play with this parameter and explore this avenue in *theory*. It is however known that, that despite living in a three-dimensional world, it is effectively possible to constrict systems of particles to two, one or zero spacial dimensions. The possibility to *physically* create "true" lower dimensional systems represents another trick played by quantum mechanics under confining potentials at ultra-low temperatures.

In some materials, it is possible to tightly confine a gas of electrons in a 2D-like sheet. At very low temperature, those confined electrons will populate the lowest available energy states, effectively entrapping them into a narrow quantum well. As all degrees of freedom tend to freeze out in the limit of zero temperature, one can in fact "completely freeze" a dimension. Physical two-dimensionality can be properly achieved provided that the temperature is low enough so the average thermal energy of the electrons is lower than the excitation energy to move along the confined direction [20]. Such systems are notoriously realized in cooled heterostructures of semiconductors, and constitute what is called two-dimensional electron gases, or 2DEG. A more detailed explanation of the heterostructures used for this research will be given in a subsequent section (see chapter 3).

1.2.4 One-dimensional systems

Starting from a 2DEG, one can also think of systems of lower dimensions. Applying electrostatic potentials can constrict the mobile electrons into one-dimensional quantum wires [23, 24], by forcing them through quantum point contacts (QPC). A QPC is a narrow constriction in a conducting material, of width in the nanometer scale, created by narrow electrostatic gating electrodes. The role of the gates is to deplete underlying electrons and to constrict their flow to a narrow channel/point. Figure 1.1 shows how depletion of the 2DEG works. A current passed through a QPC can be gradually pinched off by augmenting the (negative) gating voltage. In the quantum regime, the QPC acts as a one-dimensional waveguide for electrons. The conductance across such quantum wire is thereby quantized in units of the fundamental quantum of conductance $2e^2/h \approx 7.748 \cdot 10^{-5}\text{S}$ [24]. Increasing the gate voltage results in quantized conductance plateaus due to a depopulation of one-dimensional conducting subbands through the QPC.

As will be shown later, another example of one-dimensional structure can be found in the quantum Hall effect. In the quantum Hall regime, one-dimensional edge channels arise at the border of a 2DEG sample as a perpendicular magnetic field is turned on. Those edge states, analogous to the conducting states of a topological insulator [25], have special properties which are essential to conduct interferometry experiments.

1.3 Hall effects

As previously stated, the most famous realization of anyons is the fractional quantum Hall effect (FQHE). Thus, an investigation of fractional statistics and composite

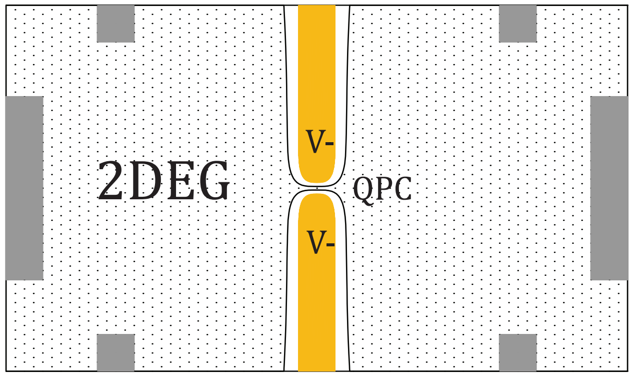

Figure 1.1: Quantum point contact (QPC) formed by depleting electrons of a 2DEG. The gates (yellow) are not in contact with the electrons of the 2DEG; an electrostatic potential repels the electrons underneath the gates, leaving only a narrow constriction for current flow. It is important to note that the gates are *on top* of the sample, so they are insulated from the electrons residing in the underlying 2DEG (Schottky barrier).

fermions first involves bringing a system of electrons in the fractional quantum Hall regime. In order to understand the role of anyons in the FQHE, we should first review the basics of the classical Hall and quantum Hall effects. It will then be easier to understand how anyons, and especially the $\nu = 5/2$ state, can be studied through interferometry experiments taking place in the FQHE.

1.3.1 Classical Hall effect

In 1879, Edwin Hall discovered that, while applying a current through a thin foil in the presence of a magnetic field, a voltage develops in the direction perpendicular to the current flow [26]. Figure 1.2 illustrates the so called classical Hall effect, in which the charges deviate towards one side of the sample, giving rise to the a net transverse potential difference. The Hall voltage is now easily understood in terms of the Lorentz force that deviates electrons as they move inside a magnetic field. The torque on the moving charges is expressed

$$\mathbf{F}_B = e(\mathbf{v} \times \mathbf{B}), \tag{1.4}$$

where $\mathbf{F}_B$ is the Lorentz force, e is the elementary charge, $\mathbf{v}$ the electron velocity and $\mathbf{B}$ the magnetic field vector. As a result of the internal charge imbalance, this Lorentz force is compensated by an electrostatic force

$$F_e = \frac{eV_H}{w}, \tag{1.5}$$

where w is the width of the sample and V_H is the Hall voltage. For a strictly perpendicular magnetic field, equating the two forces yields

$$\frac{eV_H}{w} = evB. \tag{1.6}$$

Then, the current flowing in the sample can be expressed

$$I = NevA \tag{1.7}$$

where A is the sample's cross section area and N is the electron density. We can then rearrange and express the Hall voltage as

$$V_H = \frac{wIB}{eNA}. \tag{1.8}$$

For thin samples, it is conventional to use a planar electron density, defined $n = NA/w$. The Hall voltage is therefore proportional to B and I, and related to the planar density n in the following way:

$$V_H = \frac{IB}{ne}. \tag{1.9}$$

As V_H builds up across the sample, the current I remains unaffected, meaning that the longitudinal resistance is still described by Ohms' law:

$$R_{xx} = \frac{V_{xx}}{I} \tag{1.10}$$

where V_{xx} is the voltage drop along the x-axis of the sample (see Figure 1.2). One should note that the Hall resistance R_H, being perpendicular to R_{xx}, is very often denoted R_{xy}.

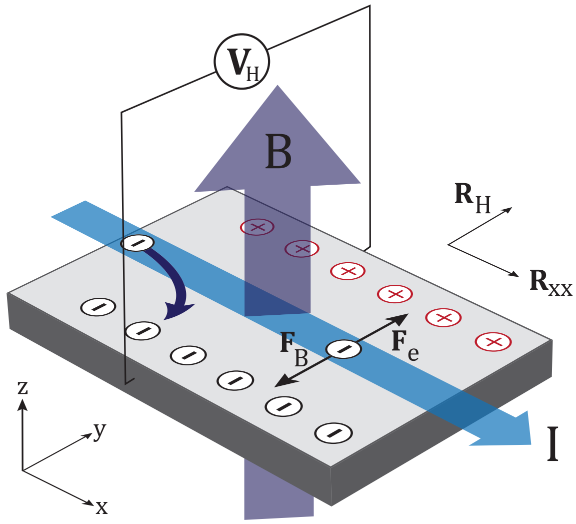

Figure 1.2: Schematic representation of the classical Hall effect. As electrons move, their direction is shifted by the perpendicular magnetic field. Their accumulation on one side of the sample gives rise to an electric field, which compensates the charge imbalance. This transverse voltage is the Hall voltage V_H. [26]

Using Ohm's law and equation 1.9, it is expressed

$$R_H = R_{xy} = \frac{B}{ne}. \tag{1.11}$$

Another useful quantity is the the Hall conductance, simply defined as

$$\sigma_H = \frac{1}{R_H} = \frac{ne}{B}. \tag{1.12}$$

In sum, the classical Hall effect describes the strictly *linear* relationship that exists between R_H and the applied magnetic field. The effect is present in normal room temperature and conditions, and does not require to be explained using quantum mechanics. The effect is incidentally put to use in magnetometers, which are probes designed to detect and measure magnetic fields. However, as presented in the next section, the linear relationship between R_H and B breaks at low temperature and in the two-dimensional limit, where quantum phenomena start to play a significant role.

1.3.2 Integer quantum Hall effect

The integer quantum Hall (IQHE) effect was first observed in 1980 by Klaus von Klitzing [27]. At low temperatures, the Hall resistance of a 2D system starts to exhibit anomalous plateaus as a function of applied magnetic field. Von Klitzing found that those plateaus coincide with vanishing resistance in the longitudinal direction (See Figure 1.3), and that they appear at values described by the relation

$$R_H = \frac{1}{i}\frac{h}{e^2} \tag{1.13}$$

where h is the Planck constant, e the charge of the electron, and i is called the *filling factor* (ν in the FQHE). The quantum Hall conductance, expressed

$$\sigma_H = i\frac{e^2}{h} \tag{1.14}$$

is therefore quantized in units of e^2/h (half the fundamental quantum of conductance).

Understanding the IQHE necessitates a two-dimensional picture, but its mechanism does not require anyons. It is rather understood as a single particle effect involving the Landau levels of the 2D system [28]. In the presence of a magnetic field, electrons confined in the x-y plane will see their energy states collapse onto quantized orbits, called the Landau levels (LLs). When solving the two-dimensional Schrödinger equation for a single electron in a magnetic field, one finds that the Hamiltonian spectrum resembles that of a harmonic oscillator

$$E_N = \hbar\omega_c\left(N + \frac{1}{2}\right) \tag{1.15}$$

with N being the energy level index and ω_c the cyclotron frequency, expressed

$$\omega_c = \frac{eB}{m^*} \tag{1.16}$$

where B is the magnetic field and m^* is the effective electron mass in the material. In free space, the Landau levels have an infinite-fold degeneracy, meaning that contain any number of states. This is however different for finite-size samples, such as those in which the IQHE is observed. For a sample of area A (area perpendicular to the applied magnetic field), one finds that the degeneracy of each Landau level is given by

$$d = \frac{AB}{he/c} = \frac{\Phi}{\Phi_0} \tag{1.17}$$

where $AB = \Phi$ is the total magnetic flux through the sample, and Φ_0 is the magnetic flux quantum [20]. Thus, there exists one energy state per flux quantum going through the sample [26]. We also notice from equation 1.17 that the degeneracy increases with magnetic field, meaning that more and more electrons are required to fill the LLs. At low temperatures, electrons occupy the lowest available energy levels, and for low B-field, the LLs are continuously filled up to the Fermi energy. But as one sweeps the B-field, the degeneracy changes, and the higher LLs gradually unload until only the lowest ones contain electrons. For some values of magnetic field, given by

$$B_i = \frac{1}{i}\frac{dh}{e}, \tag{1.18}$$

an integer number of LLs are exactly filled. The filling factor i can be seen as the ratio between the number of electrons and available states for each LL (literally how filled the levels are). In the *integer* quantum Hall effect, i is integer valued.

When the B-field has a value equal to B_i values, all lower LLs are completely filled, while higher are separated by an energy gap $\Delta = \hbar\omega_c$. At temperatures low enough such that $k_B T < \Delta$, there are really no available scattering states, meaning that the transport becomes dissipationless and the longitudinal resistance R_{xx} vanishes [26]. At exact filling, the Hall resistance becomes

$$R_H = \frac{B_i}{ne} = \frac{1}{i}\frac{h}{e^2} \approx \frac{25.813\ \mathrm{k}\Omega}{i} \tag{1.19}$$

as expressed in equation 1.13

In real systems, the LL energies are not exactly quantized. Temperature and disorder broaden the energy spectrum of each LL, and leave room for a range of states. As shown in Figure 1.3, R_H is not a perfect step function, and the conduction region of R_{xx} are diffuse (not spikes) [26, 29].

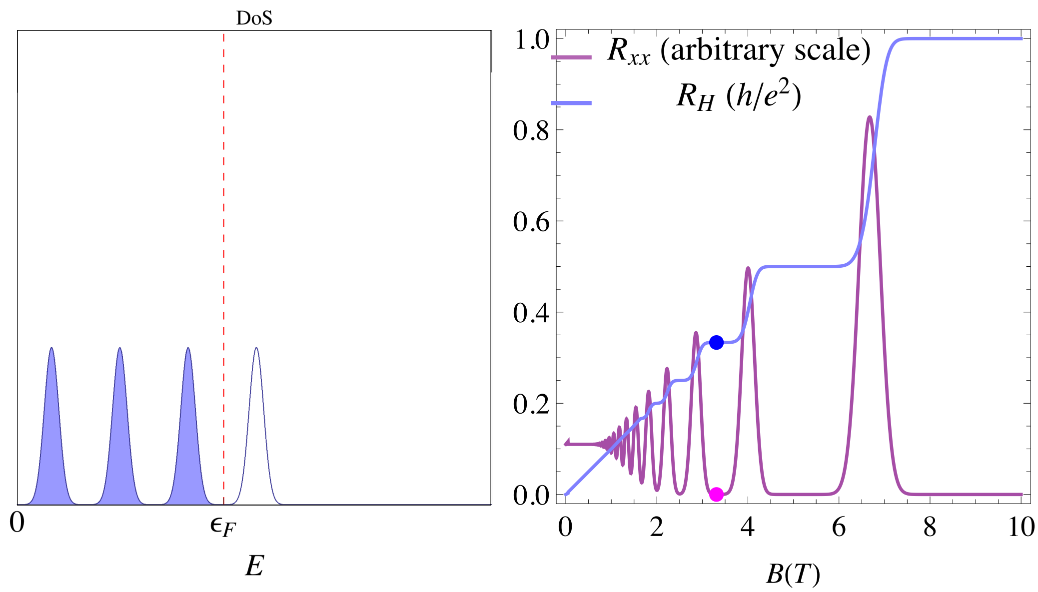

Figure 1.3: Snapshot from a *Mathematica* applet illustrating the quantization of Hall resistance R_H and vanishing of longitudinal resistance R_{xx} in the quantum Hall regime (after work by G. Jelbert and N. Walet). We see that the plateaus correspond to an integer number of Landau levels filled. As the B-field is increased, the Fermi energy sweeps across the density of states, creating a new plateau each time it crosses a new LL.

Another important feature of the quantum Hall effect is the emergence of chiral edge states at the borders of the sample. This feature is of primary importance since it provides a path through which particles can be guided, allowing for electronic interferometer geometries. Since the sample has finite dimensions, the borders act as a potential wall, forcing the Landau levels to bend upward, as illustrated in Figure 1.4. At the edges, the LLs are forced to intersect with the Fermi energy, creating one-dimensional channels along which particles are free to move. The chirality of the channels comes for the orientation of the external B-field, which forces the electrons to move in a single direction (clockwise or counterclockwise). Since the edge channels are chiral, there is a strong suppression of backscattering, which is accountable for the extremely precise conductance/resistance quantization [29].

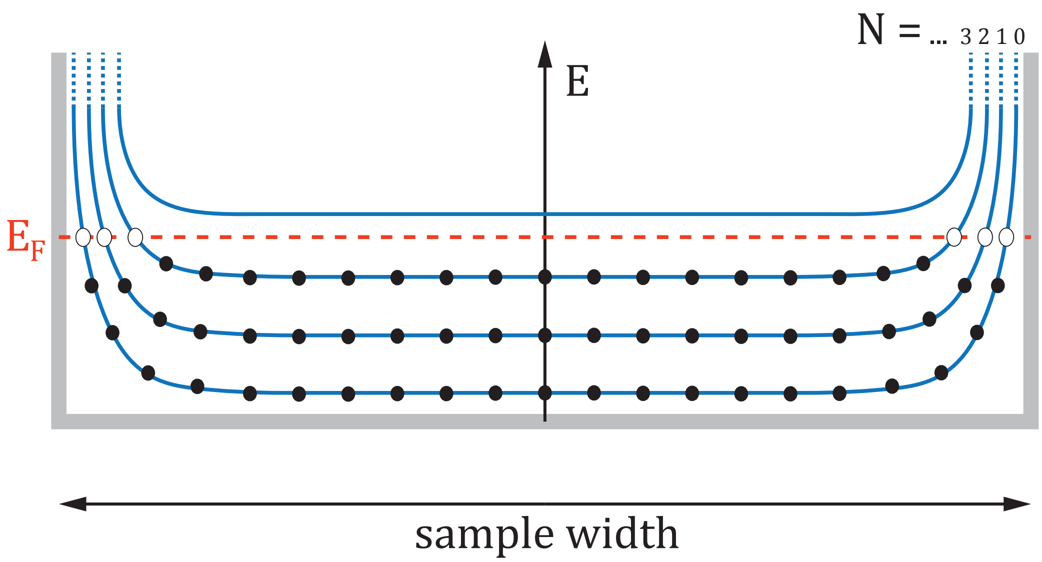

Figure 1.4: Edge channels formed at the borders of a 2DEG sample. The Landau levels (indexed N), are forced to bend upwards at the edges of the sample (it becomes increasingly difficult to push an electron "outside" the sample). As the filled LLs intersect the Fermi energy (red), conducting edge states are formed (white dots).

1.3.3 Fractional quantum Hall effect

Two year after the discovery of the IQHE, D. C. Tsui and H. L. Stormer and A. C. Gossard discovered that the quantization of the Hall conductance was in fact not limited to integer multiples of e^2/h [30]. Using samples with improved quality (higher mobility and density), they observed a *fractional* quantum Hall effect, as a plateau occurred at $\nu = \frac{1}{3}$, *i.e.* while the first LL was only one-third filled. The appearance of a plateau at fractional filling could not be explained using the usual single electron picture. The phenomenon had to be understood as a consequence of many-body interactions. Figure 1.5 shows a recent measurement of longitudinal and transverse resistances in the fractional quantum Hall regime, illustrating how plateaus emerge at fractional filling [31].

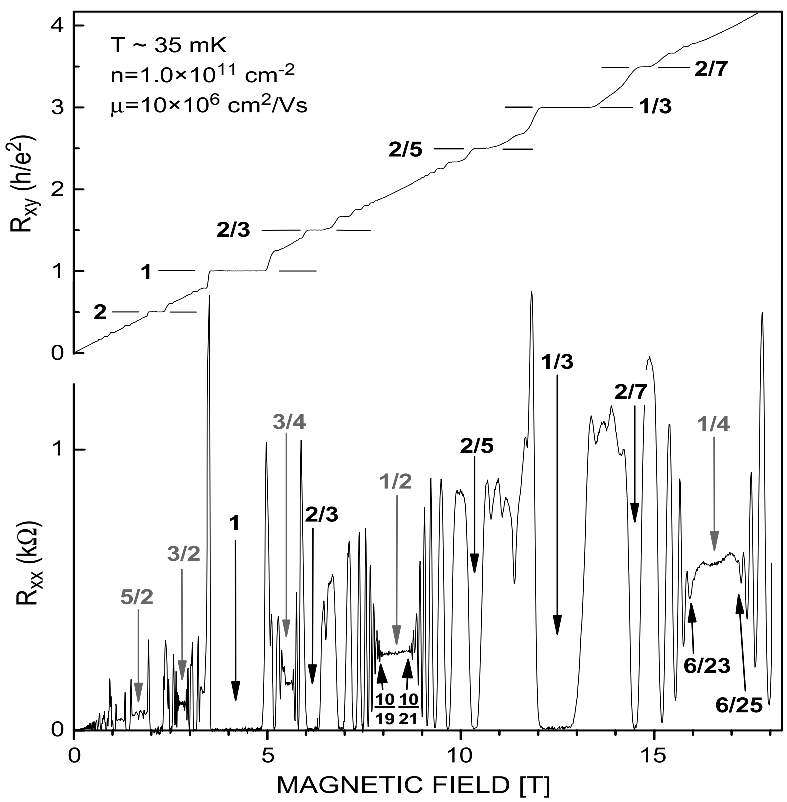

Figure 1.5: Measurements of longitudinal R_{xx} and transverse Hall resistance R_{xy} in the fractional quantum Hall regime. Plateaus in R_{xy} at integer or half filling correspond to vanishing (or minimal) R_{xx}. (Data: W. Pan, Sandia. Sample: L. N. Pfeiffer, Princeton).

To explain the FQHE, original theoretical contributions were made by Laughlin [32], Haldane [33] and Halperin [34]. The many-body ground state wavefunction suggested by Laughlin

$$\Psi_m(z_j, ..., z_k) = \prod_{j<k}^{N}(z_j - z_k)^m \exp\left[-\frac{1}{4l_B^2}\sum_j^N |z_i|^2\right] \tag{1.20}$$

where $m = 1, 3, 5...$, $z_j = x_i + iy_j$ is the location of the j^{th} particle and l_B is the magnetic length, describes quasiparticles carrying fractional charges, and explained successfully the the principal filling factors $\nu = 1/3, 1/5, 1/7...1/m$. However, a much richer set of ν values were observed (Figure 1.5), requiring a more general understanding. Haldane and

Halperin later contributed to establish the *hirarchical model*. Starting from the Laughlin states, secondary states emerge with filling factors described by the hierarchical sequence

$$\nu = \cfrac{1}{m + \cfrac{\alpha_1}{p_1 + \cfrac{\alpha_2}{p_2 + \cfrac{\alpha_3}{p_3 + \ddots}}}} \tag{1.21}$$

where $m = 1, 3, 5...$, $\alpha_i = \pm 1$ and $p_i = 2, 4, 6...$ The major upshot of the hierarchical model is that, as pointed by Halperin [34], the fractionally charged quasiparticles found in the FQHE should also obey anyonic (fractional) statistics.

The current picture, proposed by Jain [3], relies on the concept of composite fermions (CFs). A composite fermion consists of a combination of electrons and flux quanta. Recall that, in the quantum Hall regime, there is as many available states are there are flux quanta penetrating the sample. Also ν can be seen as the ratio between the number of electrons and available states for each LL. At complete filling, we had the IQHE, in which all electrons can be seen as being paired with a single flux quantum. However, in high purity 2DEGs, intermediate stable pairings can occur, corresponding to different filling fractions representing the ratio of electrons to flux quanta.

The key of the CF picture is that the FQHE can be seen as an IQHE of non-interacting composite particles in the presence of an *effective* B-field, which is different from the external applied B-Field [26]. The model interprets the FQH states as being a sequential filling of CF Landau levels around principal filling factors $\nu = \frac{1}{2m}$, yielding a general condition for strictly *odd* denominator FQH filling factors

$$\nu = \frac{p}{2mp \pm 1} \tag{1.22}$$

with integer m and p. In short, the FQHE contains fractionally charged quasi-particles obeying anyonic statistics. The anyons are two-dimensional composite fermions formed by a pairing between electrons and magnetic flux quanta.

1.3.4 FQHE at $\nu = 5/2$

The discovery of a $\nu = 5/2$ state by R. Willett *et al.* [4] challenged the composite fermions model by violating its odd denominator restriction. The occurrence of a plateau at even denominator would rather indicate a composite *boson* nature [29, 35]. The state was observed in high density and high mobility heterostructures, as a result of further improvements in sample quality [36]. In response to the discovery of the 5/2 state, the principal models suggested were the Haldane-Rezayi state [37], Moore-Read Pfaffian state [5], 331 state and later the anti-Pfaffian state [36]. Among these models, the Moore-Read Pfaffian and anti-Pfaffian have received special interest since they described a state whose excitations are expected to carry a fractional charge $e/4$, and to obey non-abelian braiding statistics. This second aspect attracted a lot of attention since Kitaev explained, in 1997, that it could be possible to use the non-abelian braiding properties of the quasiparticles of the 5/2 states to built a fault tolerant topological quantum computer [6, 38]. Non-abelian braiding statistics refers to a drastically different two-dimensional order or matter, in which an exchange of particles does not only yield an arbitrary phase shift, but a completely different state. Observing non-abelian particles would constitute a major discovery in itself, irregardless of the possible quantum computing applications.

To date, none of the previously mentioned models has been conclusively confirmed experimentally. However, using interferometry to probe the quasiparticles found in the 5/2 state could provide the elements that would confirm (or infirm) the Moore-Read Pfaffian model, depending if the observed interference patterns depict abelian or non-abelian braiding statistics. Interferometry being at the heart of this research, a detailed description will be given the following section.

The premise of the Moore-Read Pfaffian state is that the 5/2 state constitutes a Cooper-paired state of composite fermions forming a spin-polarized system [36]. Reminiscent of the Laughlin wavefunction, the Moore-Read Pfaffian wavefunction is expressed

$$\Psi_{MR} = \prod_{j<k}(z_j - z_k)^2 Pf\frac{1}{(z_i - z_j)} \cdot \exp\left[-\frac{1}{4l_B^2}\sum_i |z_i|^2\right] \tag{1.23}$$

where the Pfaffian,

$$
\begin{aligned}
Pf\frac{1}{(z_i - z_j)} \quad &\equiv \quad \frac{1}{z_1 - z_2}\frac{1}{z_3 - z_4}\frac{1}{z_5 - z_6}... \\
&\quad -\frac{1}{z_1 - z_3}\frac{1}{z_2 - z_4}\frac{1}{z_5 - z_6}... + ... - ... \qquad (1.24)
\end{aligned}
$$

is used here to represent the Coulomb interactions [36].

In short, the 5/2 state of the FQHE could be explained in different ways. Despite being strongly challenged and debated, the Moore-Read Pfaffian model remains particularly intriguing since the excitations of the wavefunction are expected to obey non-abelian braiding statistics. This feature could possibly be verified via interferometry experiments.

1.4 Anyon interferometry

In order to probe the statistics of the quasiparticles found in the $\nu = 5/2$ sate, many suggested to proceed via interferometry [8–12]. A number of experiments showed that it is possible to build anyon interferometers and measure interference, revealing the existence of fractional statistics in various states of the FQHE [13–16]. Similar investigation has already been undertaken in the $\nu = 5/2$ state [17, 18]. However, these experiments are still insufficient to rule the state as non-abelian or not, as the validity of the interference results is debated among the community.

Interference of anyons requires performing a *braiding* exchange operation, along which a phase is acquired between charges following two different current channels. In two-dimensions, braiding is the only exchange operation possible. A braiding is realized by 'winding' anyons one around the other in space and time.

1.4.1 Fabry-Perot geometry

The Fabry-Perot *optical* interferometer consists of a slab (etalon) of semi-transparent material, through which coherent light is sequentially transmitted and reflected, leading to interference. The phase picked up by the reflected light depends on the wavelength, incident angle and thickness of the slab. Tuning any of these parameters has an incidence on the interference pattern.

In a similar way, one can think of an electronic Fabry-Perot interferometer (FPI). Consider the device presented in Figure 1.6. The main idea is to use three quantum point contacts (QPCs) to deplete the electrons of an underlying 2DEG, and reshape the edge currents into an interferometer. Recall that in the quantum Hall regime, one-dimensional edge currents arise at the borders of the sample. In fact, the 'borders' of the sample are displaced by the electrostatic repulsion and we should really think of the borders as being those of the 2DEG.

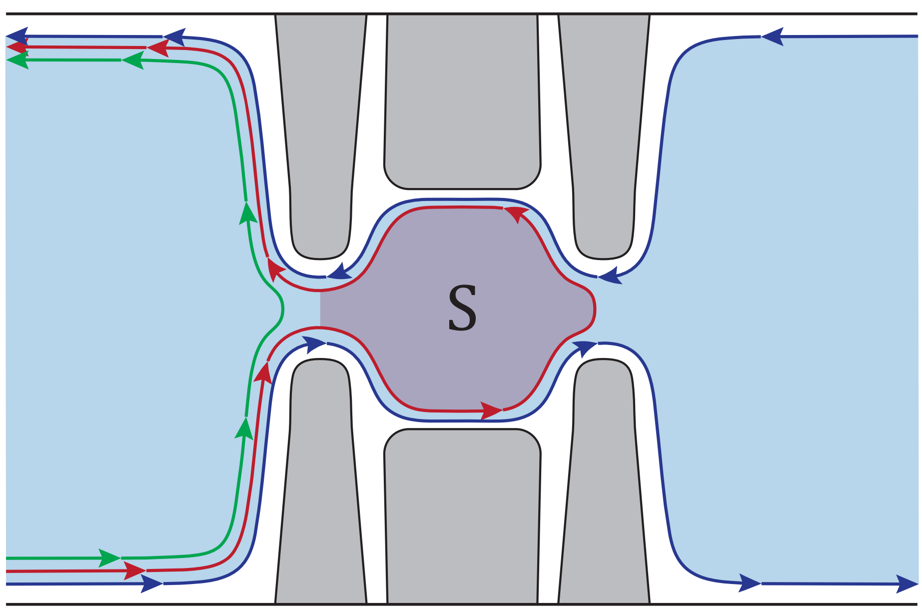

Figure 1.6: Interference between reflected (green, leftmost) and transmitted (red, encircling the central area) edge currents. The phase accumulated by the transmitted current can be tuned by a modification of the central area S. The constriction of the edge currents is achieved by QPC that deplete the 2DEG beneath the surface.

The applied voltage depletes the electrons under the gates, which can ultimately result in a characteristic 'pinch-off' of the conductance across the QPCs. If the QPCs are pinching *just right* (the exact value of the voltage will depend on each sample due to nanoscale geometry differences), the edge currents have a statistical probability of being either reflected or transmitted. Interference happens when the current transmitted to the central surface S recombines with the originally reflected current. Through this process, the current that encloses the area S accumulates a phase with respect to the reflected current.

The possibility to tune the interferometer by changing the phase accumulated around S is a consequence of the Aharonov-Bohm (AB) effect [36]. The AB effect describes phase shift that results from the coupling of the electromagnetic vector potential $\vec{A}$ with the complex phase of charged particles. In a magnetic field, the phase accumulated by a particle with effective charge e^* traveling along a path P is

$$\phi = \frac{e^*}{\hbar} \int_{\partial P} \vec{A} \cdot d\vec{r}. \tag{1.25}$$

If P defines a closed loop around an area S, then the phase difference between the transmitted and reflected currents is

$$\Delta\phi = \frac{e^*}{\hbar} \oint_{\partial P} \vec{A} \cdot d\vec{r} = \frac{e^*}{\hbar} \int_{S} \nabla \times \vec{A} \cdot d\vec{S} \tag{1.26}$$

making use of Stokes' theorem. In the simplest case, where $\vec{A}$ represents a uniform perpendicular magnetic field B, the integration becomes trivial and

$$\Delta\phi = \frac{e^*}{\hbar} B \cdot S. \tag{1.27}$$

Therefore, sweeping the perpendicular magnetic field and changing the flux enclosed in S affects the AB phase. The oscillations in measured resistance (or conductance) will have a period

$$\Delta B = \frac{\hbar(2\pi)}{e^* S} = \frac{h}{e^* S}. \tag{1.28}$$

Measuring the oscillation period ΔB can therefore indicate the charge of the quasiparticles found in the system. A second way to change the flux through area S is to change the length of the path taken by the transmitted current. Applying a more negative electrostatic potential at the central gates will deplete the central region and alter the position of the edge channel.

Reducing the area of S also offers the possibility to *expel* quasiparticles from the interferometer. Changing the number of quasiparticles encircled by the central edge current is understood as a modification of the braiding process, and has and influence on the global statistical phase acquired around S. Removing (or adding) a quasiparticle should induce a phase shift θ equal to $\nu\pi$ in the resistance oscillation pattern. Thus, as the area S is continuously constricted, one should observe a discontinuity in the resistance oscillations [36]. Changing the external B-field also has an incidence on the number of enclosed quasiparticles. At filling factor $\nu = p/q$, there are p electrons for q flux quanta. Therefore a change ΔB will result in $(\Delta B)(S) \times (pe)/(q\phi) \times (e^*/e)$ change in the number of quasiparticles within the enclosed area S [36].

1.4.2 Expected non-abelian signature

Interference of charged particles results in oscillation of measured Hall resistance, with period revealing their effective fractional charge. If the $\nu = 5/2$ state is indeed described by the Moore-Read wavefunction, then a sweep of the flux through the area S will produce oscillations corresponding to a fractional charge $e^* = e/4$. Note that this condition is necessary but not sufficient to determine whether the Moore-Read is correct, since other abelian models also predict a fractional charge $e/4$ [36].

Then, in order to verify if they obey non-abelian statistics, it is believed that one must look at the oscillation pattern as the number of quasiparticles enclosed in S is changed. In the orthodox view, if the total number (N_{tot}) of enclosed quasiparticles is even, then a sweep in enclosed flux will produce oscillations in the conductance corresponding to a fractional charge $e^* = e/4$. If the area S allows for a supplemental quasiparticle and N_{tot} becomes odd, then the oscillations should be suppressed due to the non-abelian properties (see Figure 1.7). If the quasiparticles are not non-abelian, then the oscillations should be observed at all time, independently of the parity of N_{tot} [36].

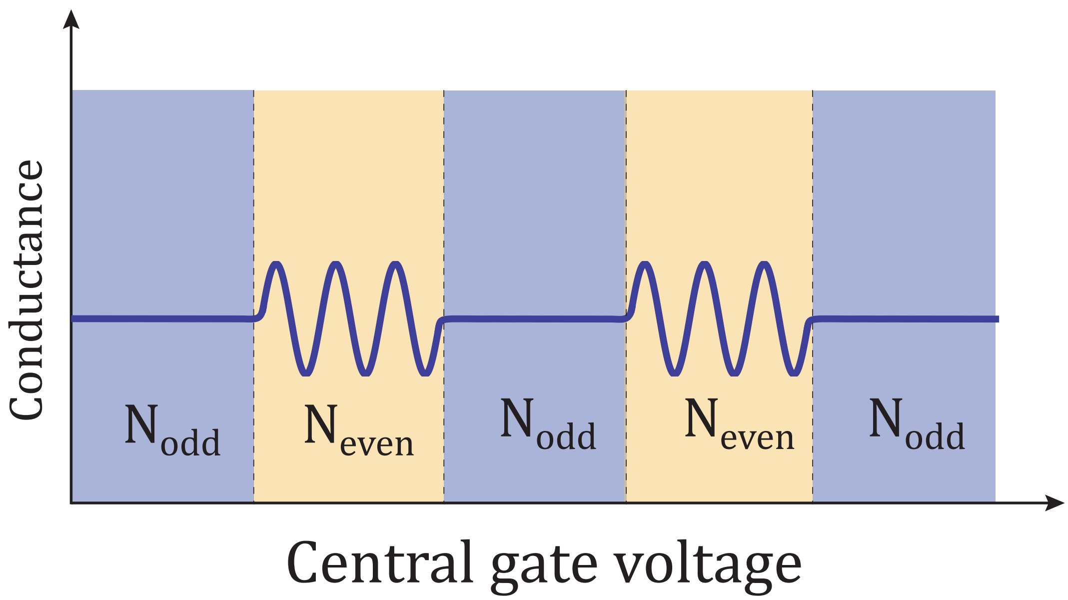

Figure 1.7: Illustration of expected aternation between oscillating and linear regimes depending on the parity of N_{tot}. As the central gate voltage (repulsive) reduces the surface S around which the AB phase is acquired, the total number of quasiparticles encircled decreases, affecting the braiding operations, in case the 5/2 state is indeed non-abelian.

Chapter 2

Technical Motivation

As stated previously, observing interference of anyons, and especially at filling factor $\nu = 5/2$, is a laborious task mostly due to the extreme fragility of the states. The most important element motivating the development of the flip-chip method is that electronic density uniformity plays a key role in the formation of robust 5/2 features [36]. Yet, the fabrication of devices (such as interferometers) to probe the 5/2 state involves several processing steps, which are likely to contaminate and alter the properties of the 2DEG. In particular, electron-beam (e-beam) lithography is susceptible to tarnish the mobility and density uniformity of the 2DEG, by trapping charges in the crystalline heterostructure. The flip-chip approach is implemented to avoid e-beam processes done directly on the 2DEG. Hence, the idea is to create an interferometer on a separate substrate, and to then flip it against the high quality 2DEG sample, as if it had initially been patterned on the latter. The following sections will review the conventional approach to fabricate gating devices on top of 2DEGs, and then illustrate the advantages offered by our innovative flip-chip method.

2.1 Electrostatic gating

Electrostatic gating is probably the most widely used technique in the modern electronics industry as it plays a role in the functioning of field-effect transistors (FETs). Gating refers to the application of a voltage (gating voltage) that is meant to affect the conductivity of the charge carriers in a semiconductor material. This principle is put to use in low-dimensional physics as well to control the flow of electrons in a 2DEG. When doing experiments to probe quantum phenomena, the scale of the gating devices (such as QPCs) must go down to micro or nanometers. To build such small devices, physicists can take advantage of nanofabrication technologies that were developed in the past decades, and perfected thoroughly thanks to the requirements of the evergrowing semiconductor industry.

2.1.1 Conventional fabrication approach

Integrated circuits composed of nanoscopic components (e.g. transistors on a CPU) are usually made via a series of lithographic interventions on a resist-coated substrate. Lithography is done by 'burning' a pattern in a very thin and uniformly spread resist, after which it is possible to develop a negative stencil of the desired device. Evaporating metal through the stencil leaves the device as if it had been printed and integrated on the substrate. In general, optical UV light is convenient and widely used for lithographic processes (photolithography). However, its main disadvantage is that the writing resolution is limited by the wavelength of light (no smaller than a few hundred nanometers). To pattern smaller devices, one has to use e-beam lithography (EBL), reportedly reaching resolutions below 5 nm [39].

EBL uses a focused beam of electrons to burn patterns in thin layers of electron-sensitive resists. The advantages comes from the fact that the de Broglie wavelength of electrons is much smaller than that of UV photons. Indeed, some EBL writing systems have accelerating voltages going up to 100 kV, meaning that electrons have a kinetic energy of about $E_k \sim 100$ keV. With rest mass of 0.511 MeV, the de Broglie wavelength of these electrons is

$$\lambda = \frac{hc}{pc} = \frac{hc}{\sqrt{2 \times E_k \times m_e c^2}} = \frac{hc}{\sqrt{2 \times 100000 \times 0.511 \times 10^6}} \approx 3.9 \text{ pm.} \tag{2.1}$$

Such resolution is in practice never achieved (for lithography or imaging), due to the size of the electron beam, to the size of atoms and resist molecules, diffusion, and other noise-inducing limiting factors. The point is that EBL is required to push the limits of top-down nanofabrication techniques, and that most groups [13–18] working on Fabry-Perot anyon interferometers take advantage of this method in order to produce devices with small enough features (area S and QPCs precise to tens of nanometers, see Figure 1.6).

The conventional method for nanofabricating gating electrodes is illustrated in Figure 2.1. First, the pattern is exposed through EBL directly on the surface of a resist-coated heterostructure, after which metal is evaporated to create the gates. But by performing e-beam lithography directly on the surface of the 2DEG, very energetic electrons might be introduced and trapped in the substrate, causing a perturbation of the 2DEG uniformity that is likely to make the 5/2 state harder −if not impossible− to observe.

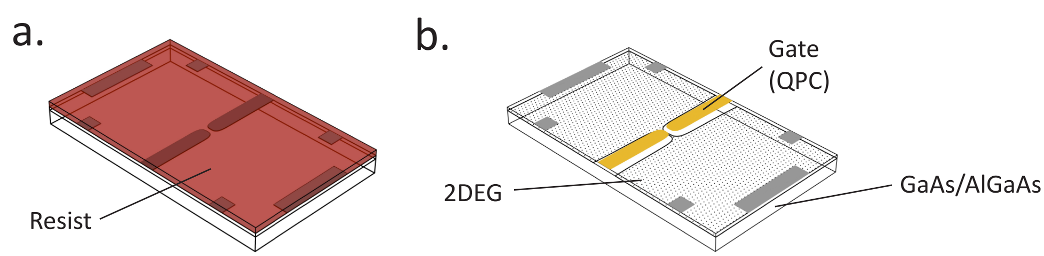

Figure 2.1: Conventional electrostatic gates fabrication method. **a.** the resist for electron-beam lithography is deposited directly on the surface of the GaAs/AlGaAs heterostructure. **b.** The metal deposition is done directly on top of the substrate. [1]

2.2 The flip-chip method

In order to avoid direct e-beam writing on the 2DEG substrates, the flip-chip method proposes to create interferometers on a separate substrate. The method, particularly suited for experiments involving ultra-high mobility samples, is currently in a patent application process, co-invented by K. Bennaceur and G. Gervais. The novelty resides in the sample assembly, where devices are held mechanically on the surface of the substrate, as opposed to being patterned directly on it.

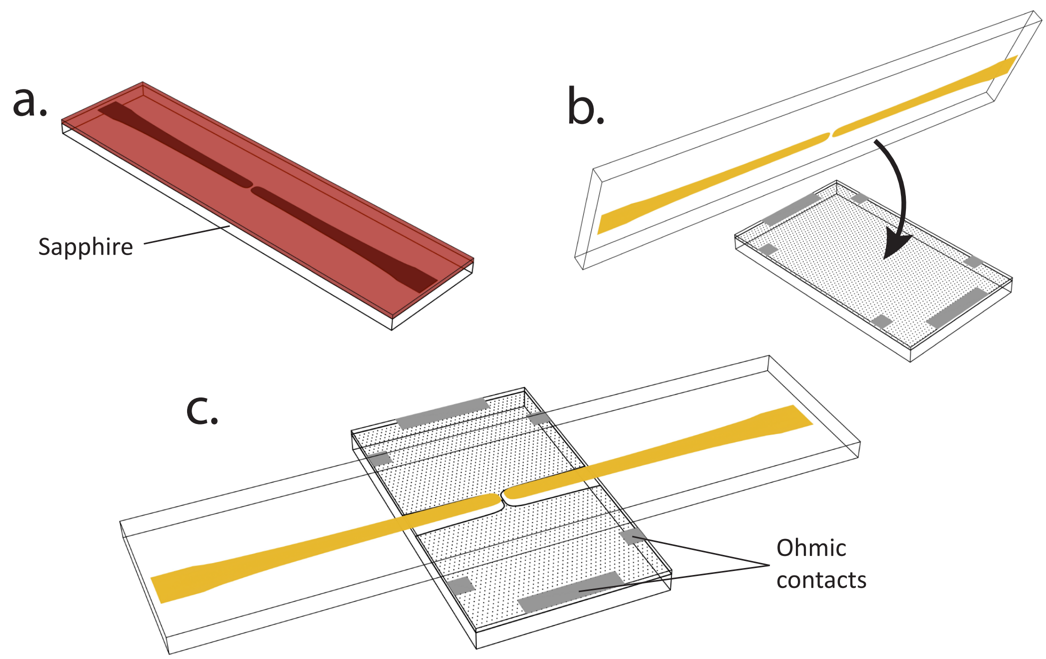

Figure 2.2: Illustration of the flip-chip concept. **a.** The metallic gates (here a simple QPC) are patterned using *e*-beam lithography on a piece of sapphire. **b.** The gates are then flipped on top of the 2DEG sample. **c.** The final assembly showing depletion of the underlying 2DEG. [1]

2.2.1 Concept and requirements

The idea of the flip-chip is, as illustrated in Figure 2.2, to fabricate the gating devices on a slab of artificial sapphire and to hold it against the 2DEG, as if it had originally been created on it. Although sapphire substrates were retained, it is relevant to say that several other candidates have also been tested in previous development phases (silicon, gallium arsenide, mica). Sapphire was kept because of its rigidity and very good electrical insulation. Moreover, using transparent materials turned out to be helpful for the assembly and testing of the flip-chip devices. Apart from making the alignment of the interferometers easier, a transparent sapphire substrate makes it possible to illuminate the underlying heterostructure with an LED during the cooldown process, which is known to improve the mobility and density of the 2DEG.

To make the flip-chip work properly, the biggest challenge comes from the fact that applying the gates mechanically on the 2DEG requires both surfaces to be *absolutely* clean and flat. Indeed, any dust could tilt the substrates, introduce a gap between the gates and the heterostructure and prevent the electrostatic voltages from correctly reshaping the 2DEG into an interferometer. The distance between the gates and the underlying 2DEG is crucial, for the dimensions of the QPC are adjusted so that the 2DEG depletion can lead to tunable narrow constrictions (see Figure 1.6). The flatness constraint also implies that the surface (top) of the metal evaporated on the sapphire has to be extremely uniform. This is only possible if the whole device is patterned *at once*, in a single *e*-beam lithography process. This fabrication challenge has been solved by using a judicious sequence of *e*-beam writing routines, allowing to expose both large and fine areas in a reasonable time (details in the following section).

2.2.2 Advantages

The ongoing efforts invested in the development of the flip-chip method are motivated by a series of advantages it has over the conventional fabrication technique (mentioned above). Despite the technical challenges associated with the implementation of the method, the the flip-chip has many positive upshots [1], the principal ones being the following:

i. **It avoids degradation of the electron mobility and density uniformity during *e*-beam lithography.**

   The bottom line argument for avoiding *e*-beam lithography is to preserve good 2DEG quality. Here, quality refers to ultra-high electron mobility (in excess of $30 \cdot 10^6$ cm^2/Vs for some of the best samples), and high density (up to $3 \cdot 10^{11}$ cm^{-3}). Those features are achieved by a meticulous layout of atomically flat semiconductors (heterostructure) grown by molecular beam epitaxy, creating the conditions for electrons to populate and move freely in a narrow quantum well. Usually, the 2DEG is situated only a few tens of nanomemters below the surface of the heterostructore sample, hence anything done on the surface of the substrate is potentially risky. It is believed that damages can be done to the heterostructure by e-beam lithography due to radiation from heating, electrostatic charging and ionization. Those risks are eliminated by doing the lithography on a separate substrate, leaving the 2DEG in pristine conditions.

ii. **It avoids degradation of the electron mobility and density uniformity during metal evaporation.**

Metal evaporation (sputtering or physical vapor deposition) is a process through which metal atoms such as gold, aluminum, titanium or nickel are deposited on the surface of a substrate in order to create contacts or gates. The evaporated atoms are ejected from nearly boiling metal (in vacuum) and thus reach the surface of the sample with a relatively high velocity. The atoms deposited on the surface of the heterostructure can possibly disturb the delicate semiconductor layout, introduce impurities and cause density and mobility variations in the 2DEG. Those impurities, being in the neighborhood of the mobile electrons, could also interfere with the edge channels of the interferometer.

iii. **It avoids contamination by chemicals throughout the nanofabrication processes.**

The fabrication of gating devices involves steps during which various chemicals are put in contact with the substrate. The chemicals, such as resist (PMMA) and solvents (acetone, isopropyl alcohol, methyl isobutyl ketone) can be hard to remove completely (that is to say, with absolutely no molecules left on the surface of the substrate). The residues, if any left, could trap charges and cause fluctuations in the 2DEG electron density, and interfere with the interferometer QPCs fine-tuning.

iv. **It reduces strain and stress caused by differential thermal contractions.**

The bulk of the heterostructures, made out of GaAs, and the various metals used for the gating devices have different coefficients of thermal contraction. When cooling down the samples, this difference can cause strain in the materials and possibly alter the performance of gating devices (phenomenon known as differential contraction). Once again, flatness is of prime importance, and it is safer to avoid strain on the heterostructure in order to preserve the integrity and quality of the 2DEG.

v. **It makes it possible to reuse the 2DEG materials and interferometers.**

Nanofabrication of complex devices often has a low yield and requires many tests before reaching success. By fabricating the devices on a separate substrate, it is possible to save the precious 2DEG material. Furthermore, the flip-chip method makes it possible to easily test different regions of a same 2DEG sample. This is a great advantage since it is known that the electronic density of ultra-high mobility samples can vary between different parts of the wafer.

Chapter 3

Methodology

Although anyon interferometry opens a door through which intriguing new physics could be observed, the challenges behind the flip-chip interferometers are firstly technical. Indeed, the heart of the project resides in the implementation of a new technique for probing ultra-high mobility samples in a non-invasive manner, in order to keep the delicate 2DEGs in pristine condition. This chapter will present the fabrication steps of the flip-chip Fabry-Perot electron interferometers, and provide a description of the equipment used to test them. Purposefully technical and detailed, the following sections are intended to document the elaboration of the devices as well as possible, thereby allowing future researchers to keep moving forward in line with this project.

The fabrication of the flip-chip interferometers contains three main steps: the nanofabrication of the interferometers themselves, the preparation of the contacts on the 2DEG samples, and finally the assembly of the two previous elements onto a flip-chip sample holder. The samples are then tested via standard low-noise measurements taking place at cryogenic temperatures.

3.1 Nanofabrication

The Fabry-Perot interferometers are fabricated by e-beam lithography and metal evaporation on sapphire substrates. In order to avoid contamination from dust particles, all nanofabrication steps are accomplished in a cleanroom (class 1000). Beyond standard nanofabrication procedures, the cleanness of the samples is of paramount importance for the flip-chip devices since two surfaces (interferometer and 2DEG) will have to be put in contact perfectly. Flatness is a key factor and contamination should be avoided at all costs.

3.1.1 Interferometer design

The first step of the fabrication process is to draw the interferometer using a CAD software. The *e*-beam lithography software interprets the CAD drawings and traces it by controlling the beam of and electronic microscope. Even at minimum magnification, the writing field of most electronic microscope is limited to a few mm^2. As stated above, the flip-chip method requires to expose the whole pattern at once, so the metal must be evaporated uniformly over the whole interferometer. The drawing must therefore be broken into many layers, which will be exposed sequentially, at different magnifications and beam intensities.

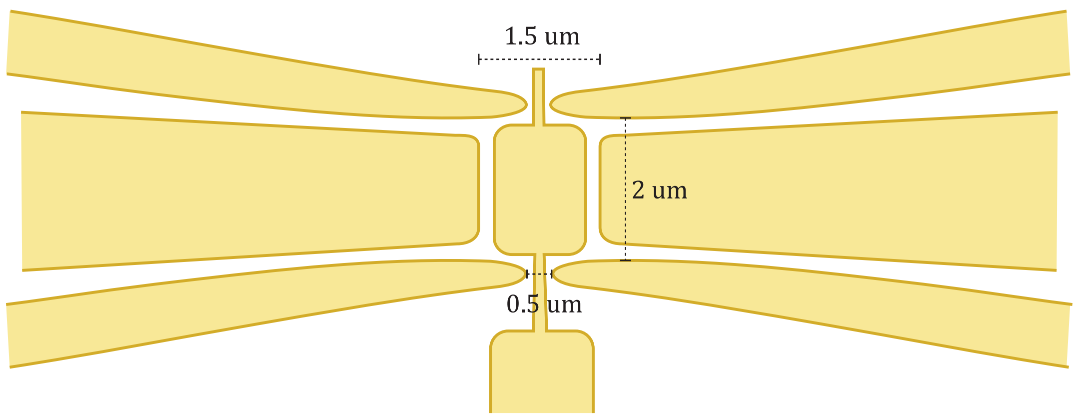

Figure 3.1: Schematic drawing of the central part of the top-gated interferometer.

The most important part of the interferometer consists of three central QPCs with a topgate (Figure 3.1 and 3.2). The QPCs (with separation of 500 nm) are followed by long tracks leading to contacts (300μm×300μm), on which wires will later be bonded (see whole pattern in Figure 3.6). The role of the top gate is to apply a uniform electrostatic potential on top of the area S of the interferometer, allowing for a fine tuning of the electronic density within S and, importantly, to ensure that the interference of charged particles happens in the Aharonov-Bohm regime by screening coulomb interactions.

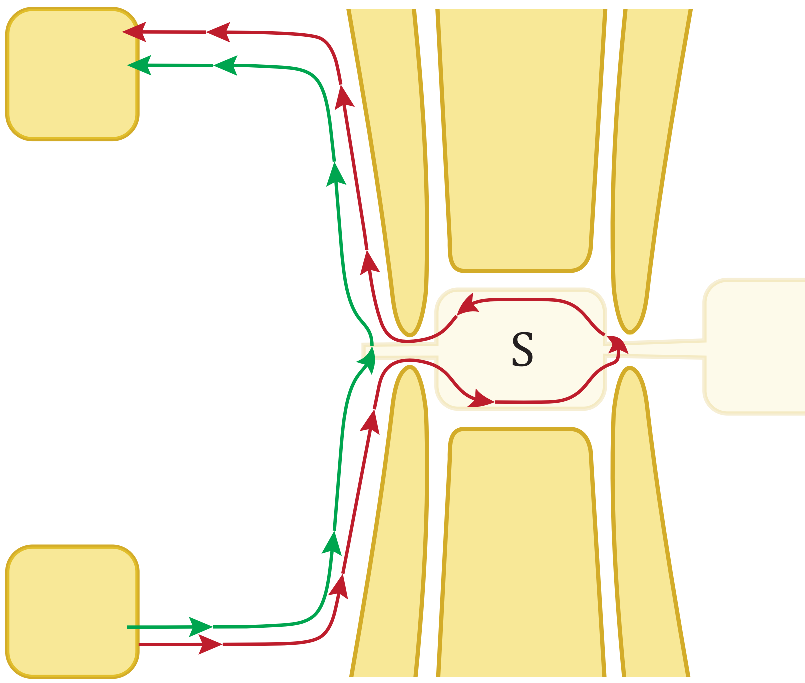

Figure 3.2: Schematic drawing of the edge currents interference in the Fabry-Perot design. The edge current arriving at the leftmost QPC is either reflected (green) or transmitted (red). The area S encircled by the transmitted edge current can be adjusted by changing the voltage applied on the central gate.

In order to have enough resolution to draw the smaller features of the interferometer, the central pattern is done first, followed by a succession of increasingly bigger patterns. The bigger layers (Figure 3.5-3.6) are written with higher beam current and lower magnification, as the resolution of the contact leads is not critical (they only have to carry voltage to the QPCs).

The rationale behind the actual *dimensions* of the Fabry-Perot interferometers stems from the ultimate goal to observe interference of quasiparticles in the 5/2 state of the

FQHE. Indeed, from equation 1.28, one expects to measure oscillations in B-field with period $\Delta B = h/e^*S$. The 5/2 state contains quasiparticles with fractional effective charge $e^* = e/4$. Furthermore, the "width" of the 5/2 R_{xx} dip is relatively narrow compared to other fractional states. Estimating that it would be convenient to observe around 20 periods ΔB within that dip of ~ 0.2 T, one can extract that an approximate surface S of $\sim 1.6 \times 10^6$ nm^2 is required at the center of the interferometer. This is approximately the half the dimensions of the central area depicted in Figure 3.2, which leaves enough room to tune the dimensions of S to the right value.

3.1.2 Electron-beam lithography

As stated above, the flip-chip method requires the whole interferometer to be flat, so the metal evaporation must be done at once on the whole surface. This is a bit unconventional since e-beam lithography (EBL) is usually employed to achieve high resolution, and not to expose large surfaces. The critical parts are normally fabricated using through EBL and metal evaporation. The contacts are *then* created using alignments masks and photolithography. Using both EBL and photolithography forces the evaporated metal layers to overlap oven some small area. This method cannot be use in the flip-chip case. The solution is to use extremely high beam current settings on the microscope in order to expose large areas in a short time. Since the lithography is done on separate substrate, a high beam intensity will not damage the 2DEG.

The substrate chosen to support the interferometer is sapphire (Al_2O_3), because of its great insulating properties which avoid leaks and shorts as gating voltage is applied, its flatness, its rigidity, and its transparency. The latter property is used to check the flatness of the flip-chip, align the interferometers on the 2DEG and illuminate the heterostructure with an LED during cooldowns. However, performing high resolution EBL on a very well insulating substrate is not an easy task. Indeed, charges from the beam accumulate in the substrate if they are not evacuated properly during the writing, resulting in disastrous distortions of the drawing. To prevent charge accumulation during the e-beam writing (and later accidental electrostatic discharges between the gates), a 45 nm sacrificial layer of chromium is first deposited on the sapphire substrate

(Figure 3.3 and 3.4). The layer will be etched after the metal evaporation step, otherwise the gates would remained electrically connected.

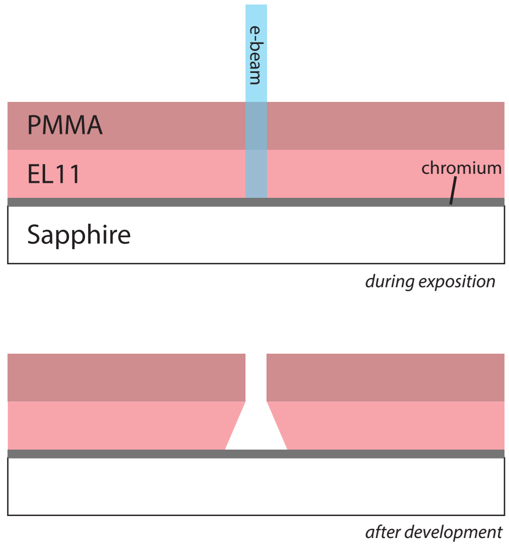

Figure 3.3: Illustration of a bi-layer EBL process with underlying chromium layer. The EL11 resist is more sensitive than the PMMA, meaning that it will be more affected by the same exposure dose. This facilitates the lift-off after metal deposition. The chromium layer (45nm) helps to evacuate the charges during the e-beam writing.

Then, the sapphire substrate is coated with an electron-sensitive resist. For direct write e-beam, a superposition of poly(methyl methacrylate) (PMMA) and poly (methacrylamide) copolymer (PMMA-co-PMAA) of type EL11 are used. The latter is slightly more sensitive than PMMA, which means that a same exposure dose will have a stronger effect on it. By spreading EL11 under PMMA, the development of exposed areas will leave a cavity, making it easier to detach the residual metal and resist afterwards. Figure 3.3 illustrates this layered technique. The resist spin-coating recipe is the following, resulting in a final thickness of approximately 1400 nm.

- Sapphire wafer is cut into samples of 11×10 mm, then cleaned with water.
- In the cleanroom, a 45nm layer of chromium is deposited using a NexDep Ebeam Evaporator.

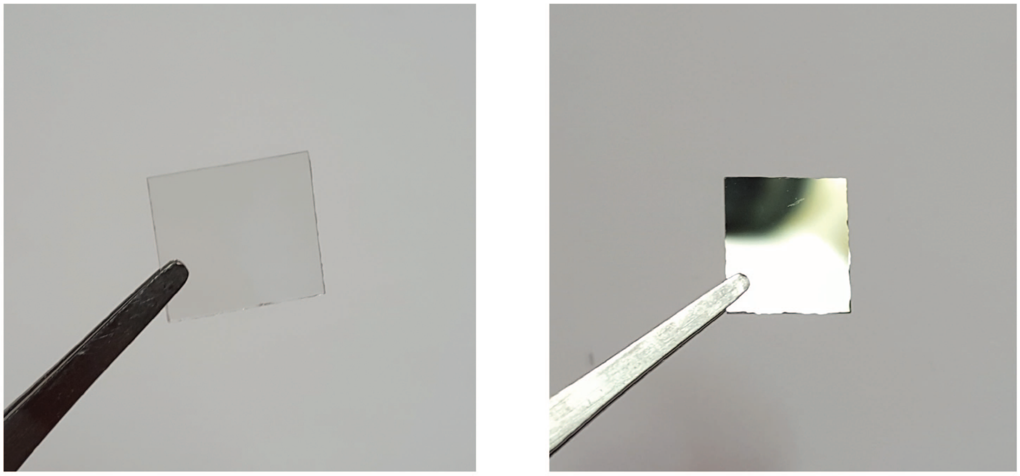

Figure 3.4: Picture of a 11×10 mm sapphire substrate before (left) and after (right) the 45 mm chromium layer deposition.

- The samples are cleaned in acetone, isopropyl alcohol (IPA) and then water.
- The samples are *prebaked* (dehydrated) for 5 minutes at 150°C.
- The samples are spin-coated with MMA(8.5)MAA EL11 at 2000 rpm for 45 seconds, then immediately softbaked for 90 seconds at 180°C on a hot plate.
- The samples are spin-coated again, this time with PMMA A7 at 4000 rpm for 45 seconds, and immediately softbaked for 90 seconds at 180°C.

The EBL writing routine is implemented in a software (eLine Plus) controlling the beam and stage of a 30kV Raith Gemini electron microscope (operated at Polytechnique Montreal). Figure 3.5 and 3.6 illustrate how the pattern is divided. The layers of the CAD pattern are independently treated, with customized magnification, beam settings and doses ranging between 150 and $250\mu\text{C/cm}^2$. The central region of the interferometer (requiring highest resolution) is done at high magnification (1000x) and low beam current (110 pA). Then, the microscope zooms back to fit the successive layers, using increasing beam currents to accelerate the process. For large areas, the doses are purposefully higher than required to make sure that they are exposed sufficiently. The largest layers are done in wide-field mode (~50x) using the highest available beam current (~10 nA). In this last step, the software needs to move the stage of the microscope, as even the lowest magnification limits the field of view to about 3×3 mm, which is still too small to fit the 8 mm long interferometers. The total exposition routine takes about 15 minutes per interferometer, most of the time being used to expose the large contacts and leads.

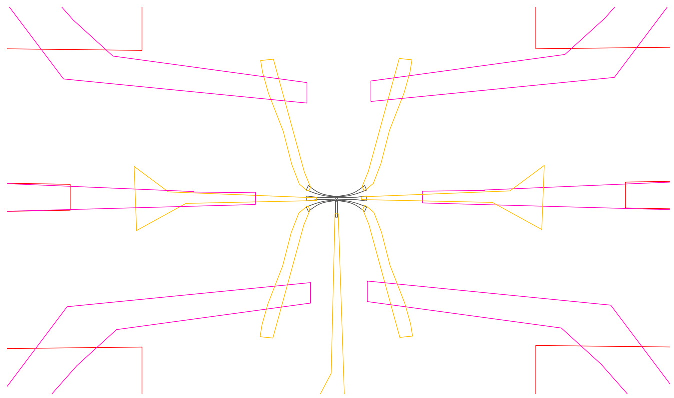

Figure 3.5: Drawing of the central region of the interferometer, showing the different layers used to link the contacts to the QPCs and topgate. The overlap of the different layers is purposefully exaggerated since offsets between layers can occur within the lithography writing routine.

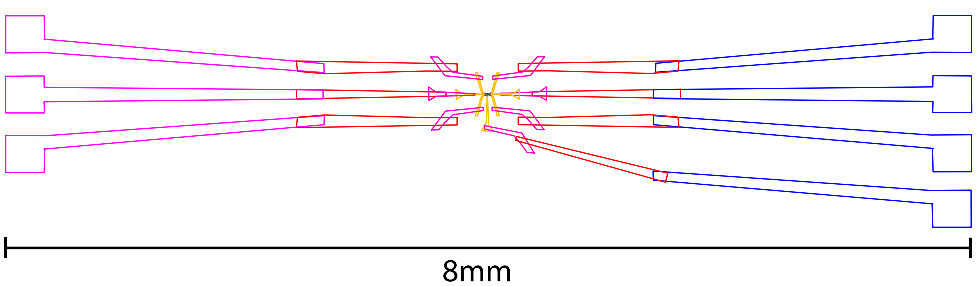

Figure 3.6: Complete drawing of the Fabry-Perot interferometer (real proportions), showing all contacts and leads going to the QPCs. The whole interferometer is 8mm long. Again, overlap regions are introduced to prevent offsets.

3.1.3 Metal deposition

Once EBL is done, the resist is developed in order to create a "stencil" through which metal can be deposited (see Figure 3.7). The development of PMMA and EL11 takes place in methyl isobutyl ketone (MIBK), an organic solvent that dissolves the resist where the patterns were exposed to the e-beam. The method is the following:

- In the cleanroom, a mixture of 1:3 MIBK/IPA is prepared.
- The samples are immersed in the mixture and agitated for 30 seconds (or slightly longer if needed).
- The development is stopped in water.
- The samples are dried using a delicate nitrogen gun.

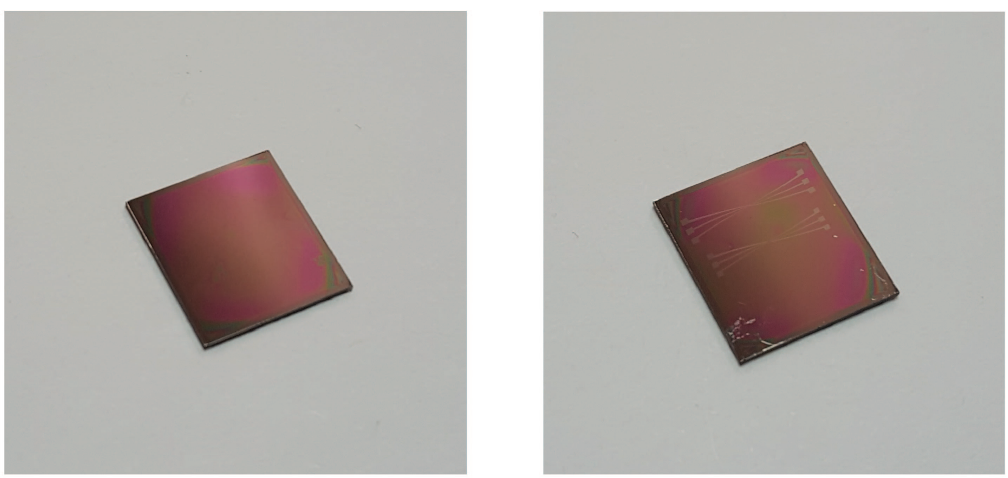

Figure 3.7: Pictures of a sapphire substrate on which was applied electron-sensitive resists (EL11 and PMMA). The left picture shows a sample just after spin coating, before EBL. The sample on the right has EBL patterns, visible after development.

After development, the samples are ready for metal deposition. The interferometers are made from a superposition of titanium and gold. Applying a fine layer of titanium will improve the adherence between the sapphire and metal. The bulk of the interferometers consists of a thin layer of gold, a good conductor immune to oxidation. The deposition steps are:

- Deposition of 7 nm of Ti, once a good vacuum is reached in the chamber of the NexDep Evaporator

- Deposition of 150 nm of Au.

After metal evaporation, the whole samples are covered in metal. To leave only the interferometers on the surface of the sapphire pieces, another solvent is used to dissolve the resist that remains underneath, thereby washing away all undesired metal. The lift-off process is done in a bath of heated (70°C) Microposit Remover 1165 *without* ultrasounds as those can damage the finest parts of the interferometers, in which the samples are left for about one hour. The interferometers are then delicately washed with IPA/water and dried with nitrogen.

3.1.4 Chromium etching and cleaning

At this point, the interferometers rest on top of the thin chromium layer. The chromium must be removed in order to disconnect the gates. To do so, the samples are cut and immersed *individually* in Transene Chromium Etchant 1020, until it disappears from the sapphire substrate. A constant monitoring is primordial, since leaving the samples in the solution for too long could etch the chromium underneath the interferometers and detach them from the sapphire. After etching the chromium, the interferometers are rinsed in water. This final etching also ensures that the samples are deprived of any residual resist and dust particles. Figure 3.8 shows an example of finished interferometer.

3.1.5 Atomic layer deposition

Leaks are a problem often encountered when using electrostatic gates: once the flip-chip are assembled and tested, the applied electrostatic voltage can produce a small current through the heterostructure and reach the 2DEG. Furthermore, shorts can occur

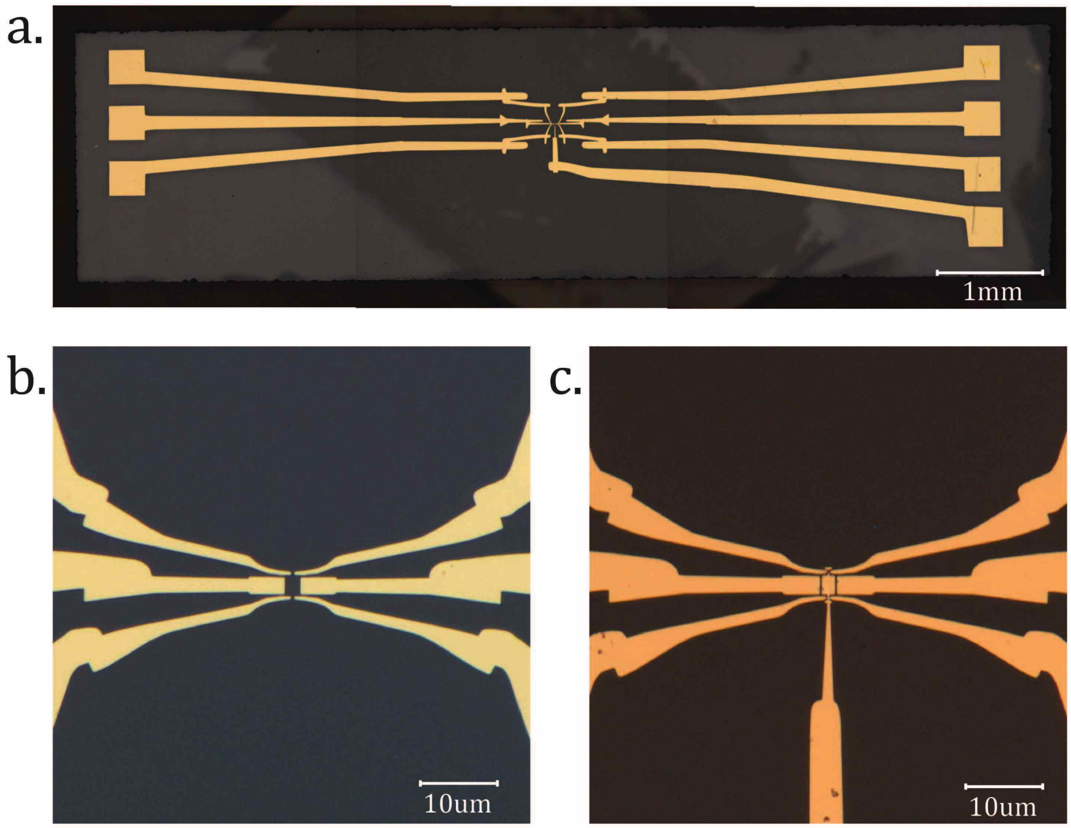

Figure 3.8: Optical microscope pictures of a completed interferometer. **a.** Whole interferometer after chromium etching. **b.** Zoom of the central region of an interferometer (no top-gate design). **c.** Zoom of the central region of the interferometer shown in a. (sample by K. Bennaceur.)

between the gates themselves, being separated by only a few hundreds of nanometers. In order to prevent any leakage, the devices are covered with an insulating substance. Each interferometer receives between 30 and 100 nm of Al_2O_3 through atomic layer deposition (ALD). This is effectively entrapping the interferometers in a shield of sapphire, preventing electric discharges and leaks. This sapphire coating should not alter the flatness of the interferometers as the layer is grown evenly, conforming to the shape of the devices.

3.2 Two-dimensional electron gases

The second part of the fabrication process is the preparation of the 2DEG samples. This research was conducted using various 2DEG materials. Most of the preliminary tests and proofs of concept were made on 2DEGs fabricated at Sandia National Laboratories (NM), supplied by our collaborator J. L. Reno. These 2DEGs have a great electron mobility ($\sim 2 \times 10^6 \text{cm}^2/V \cdot s$), but still not high enough to allow for the emergence of the $\nu = 5/2$ state. The ultra-high mobility 2DEGs (in excess of $30 \times 10^6 \text{cm}^2/V \cdot s$) used to study the 5/2 state are obtained through a collaboration with L. N. Pfeiffer (Princeton). The rarity of those 2DEG samples is part of the motivation behind the development of the flip-chip method, hoping to be able to reuse the precious materials.

3.2.1 Heterostructures

The 2DEG materials used for this study are gallium arsenide (GaAs) and aluminum gallium arsenide (AlGaAs) heterostructures grown by molecular beam epitaxy (MBE). MBE is a slow growing process through which atoms are gradually incorporated to the surface of a substrate. Under the right conditions, this growing technique yields nearly perfect crystals (defect-free), with atomically flat precision. The heterostructures are engineered by means of a judicious superposition of semiconductor and dopant layers, which produces an alteration of the band structure that confines electrons into a narrow quantum well. At low temperatures, all mobile charges are trapped in this planar well, creating a two-dimensional gas of electrons. Sophisticated growing recipes yield 2DEGs with phenomenal mobility (up to 35×10^6 cm^2/Vs for the best samples from L. N. Pfeiffer).

3.2.2 Ohmic contacts

The 2DEG wafers are first cut into pieces of about 5×8 mm. The pieces are *cleaved* manually without using a rotating blade, being careful not to scratch their surface. This precaution ensures that there is no contamination by microscopic GaAs dusts. Indeed, those can be nearly impossible to remove due to Van der Waals interactions with the crystal's surface. Once again, flatness is primordial for the proper functioning of the flip-chips.

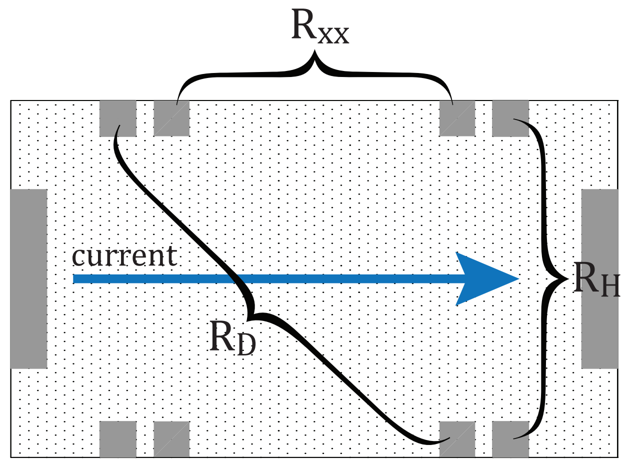

Figure 3.9: Drawing of ohmic contacts (grey) evaporated on top of the heterostructure. The number of contacts on each sides of the 2DEG sample multiplies the possible measurement configurations. Current is flown for any contact on the left of the sample (so, to the left of the interferometer). Ground is connected to any contact on the right.

The contacts are disposed according to the standard design shown in Figure 3.9, leaving room for different combinations of R_{xx}, R_H or $R_{xx} + R_H = R_D$ measurements. They are created by metal evaporation through a *shadow* mask, a fine metallic stencil placed delicately on top of the 2DEG samples. The shadow mask method is used to avoid performing UV lithography on the 2DEG samples, leaving them as pristine as possible. The contact recipe goes as follows:

- Evaporation of Germanium/Gold/Nickel/Gold with thicknesses of 26/54/14/100 nm.
- Annealing (JetFirst 200) in forming gaz, mixture of hydrogen and nitrogen, for 60 seconds at 420°C.

The annealing step is essential to diffuse the metals through the GaAs surface. Indeed, since the 2DEG is below the surface in the heterostructure, the conducting metal atoms must be forced through about 50 nm of semiconductor material. By ramping up the temperature, the atoms can diffuse and reach the 2DEG, effectively creating ohmic contacts. Figure 3.10 shows a picture of completed 2DEG sample, with contacts, ready to receive a flip-chip interferometer.

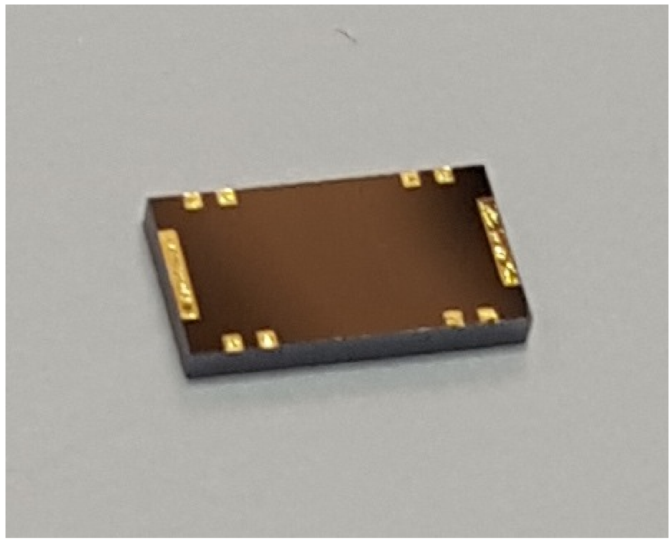

Figure 3.10: Picture of a typical 2DEG sample with ohmic contacts created by metal deposition and diffusion.

3.3 Flip-chips

3.3.1 Assembly

The interferometers are held on top of the 2DEGs substrates using very soft mechanical springs made of BeCu pressing on a sapphire top plate, as illustrated in Figure 3.11. Screws are passed through the springs before being inserted in threaded holes made in the G10 epoxy laminate printed circuit board (PCB). Apart from the customized borders leaving space for the screws, the holder is a normal 16-pins PCB.

Since flatness is of critical importance, the assembly is done in cleanroom environment to prevent any dust from contaminating the surfaces that will be put together. First, gold wires are connected to all contacts of the 2DEG and interferometer using

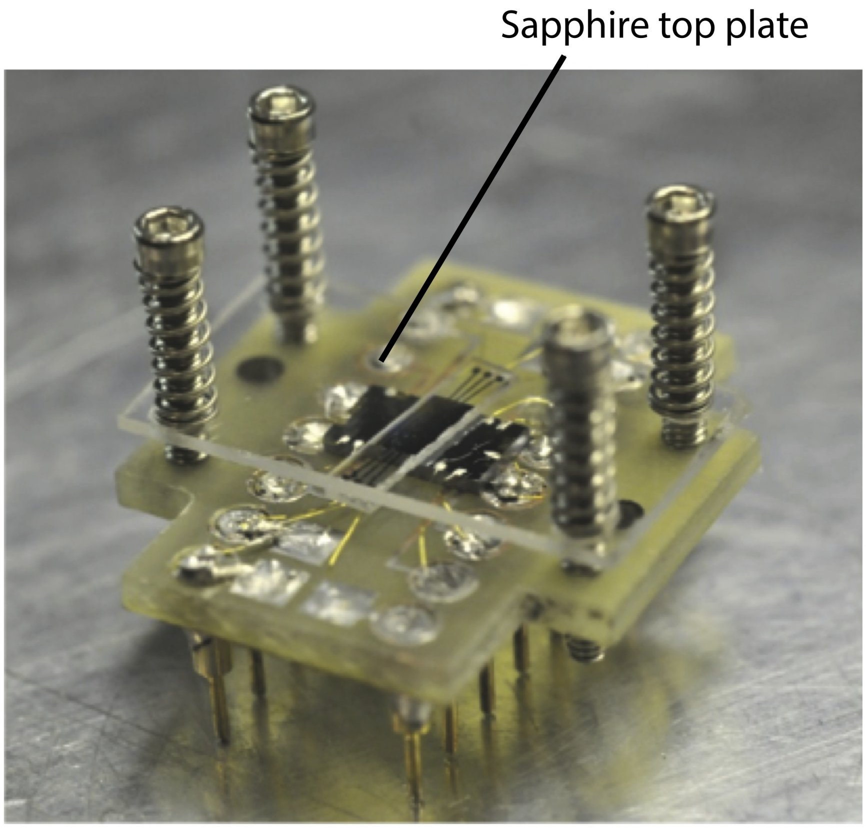

Figure 3.11: Photo of a flip-chip interferometer mounted on a PCB sample holder. The springs maintain the sapphire top plate against the back of the interferometer, holding all the pieces mechanically. [1]

silver epoxy. To protect the samples, the PCB holder is maintained on a custom made grounded copper mass, whose role is to evacuate charges in case of accidental electrostatic discharges. While the 2DEG is resting flat on the PCB, the interferometer is then delicately placed on top, followed by the top plate and screws. The gold wires are finally soldered with indium to the contacts of the PCB.

3.3.2 Flatness verification

Using a transparent material (sapphire) for the flip-chips offers two advantages during the assembly: it is easier to align the interferometers on the 2DEGs, and it is possible to verify the flatness of the flip-chip using light interference. Indeed, placing two plates of transparent material one against the other will result in Newton rings, as illustrated in Figure 3.12.

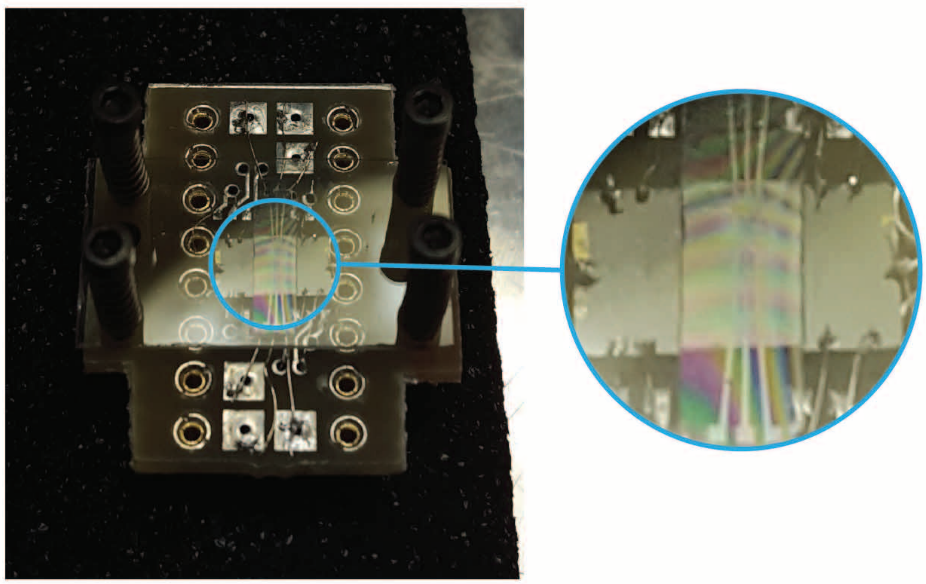

Figure 3.12: Newton rings pattern formed by the interference of light reflected by two surfaces separated by a very thin layer of air in the assembled flip-chip. Multiple stripes indicates that the flip-chip is not perfectly flat, but it can be fixed by delicately balancing the pressure through the four screws and springs.

The periodicity of the pattern is related to the wavelength of the light reflected, and indicates a tilt between the surfaces. If there is *no* tilt, then the color of the interference pattern should be uniform everywhere between the plates. This principle can be applied to the thin interstice between the 2DEG and the interferometer. If there is no dust and the interferometer is completely flat, then there should be no fringes (only one uniformly distributed color). It is possible to tune the flatness by *gently* adjusting the screws holding the flip-chip in place. If a dust particle is detected (a point causing many small Newton rings), then the flip-chip must be unmounted and cleaned.

3.4 Electronic transport measurements

Fractional quantum Hall and anyon interference measurements must be performed at ultra low-temperatures and require using low-noise techniques. Before attempting anyon interferometry, the first step is to verify that all three quantum point contacts of the interferometers can produce a characteristic pinch-off in conductance. This feature is essential, as explained above, to make the interferometers work. Before a complete pinch-off, the QPCs should behave like quantum wires, in which conductance is quantized in units of $2e^2/h$. Observing this behavior is important to ensure that the QPCs function properly in the quantum regime, where a fine tuning of gate voltage will be essential for the interferometry experiments.

3.4.1 Measurement circuit

The main difficulty when measuring quantum wires or QPCs comes from the fact that the resistance of these devices usually varies over a very large range during the course of an experiment. At low temperatures, the 2DEG offers very little resistance. But as the gate voltage constricts the flow of electrons, the conductance across the QPC enters the quantized regime, meaning that resistance reaches values up to $h/2e^2 \approx 12.9$ kΩ. The usual approach for such measurements is to use low frequency AC signals from lock-in amplifiers.

Figure 3.13 shows a diagram of a 2-point probe circuit used to measure conductance across interferometer QPCs. The lock-in amplifiers being operated at 5 V, it is possible to measure the voltage drop across a resistor in series with the sample, from where the conductance through the sample can be calculated. Measurement of the voltage drop across the 2DEG is accomplished using Stanford Research Systems SR830 lock-in amplifiers at a frequency of about 100 Hz or below. (An additional lock-in can also be added for 4-point probe measurements.) The gating voltage that will pinch the conductance is applied by a Keithley 2400 general purpose sourcemeter.

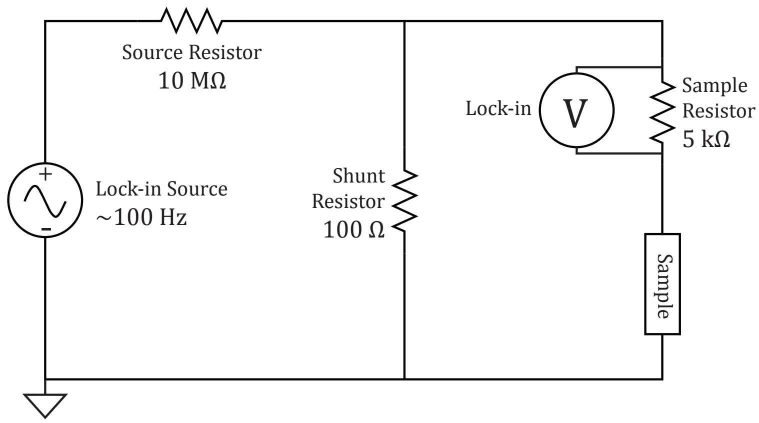

Figure 3.13: Circuit used to measure the voltage drop across the 2DEG as the gates constrict the flow of electrons (2-points). [40]

3.4.2 Low temperature fridges

Low temperatures are required to observe both the quantization of conductance and the FQHE. The measurements are conducted mainly in two cryostats: the *Variable Temperature Insert* (VTI) and a *Janis JDR-150* dilution refrigerator. The VTI is a smaller refrigerator designed for preliminary testing, usually employed with liquid nitrogen (LN2). It is used in order to verify if the samples work, i.e. if the QPCs can pinch-off the conductance across the 2DEG. Working samples are then moved to the Janis dilution refrigerator where a magnetic field can be applied, cooling down to temperatures below 20 mK .

The VTI works with liquid helium or nitrogen, and offers working temperatures ranging between 1.5 and 300K [40]. It is particularly convenient insofar as the insert (holder connecting the sample to the external instruments through wiring) can be removed and replaced *while* the cryogenic liquid is still inside. Efficient testing of multiple samples can therefore be achieved during a single LN2 transfer. The VTI cooling is done by pumping on nitrogen gas flowing through the sample chamber. The LN2 reservoir is in contact with the sample chamber only though a needle valve (see Figure 3.14). While pumping on the chamber, LN2 is slowly allowed through the valve. As it fills the vacuumed space, the high energy molecules are evacuated, resulting in a drop in temperature (evaporative cooling).

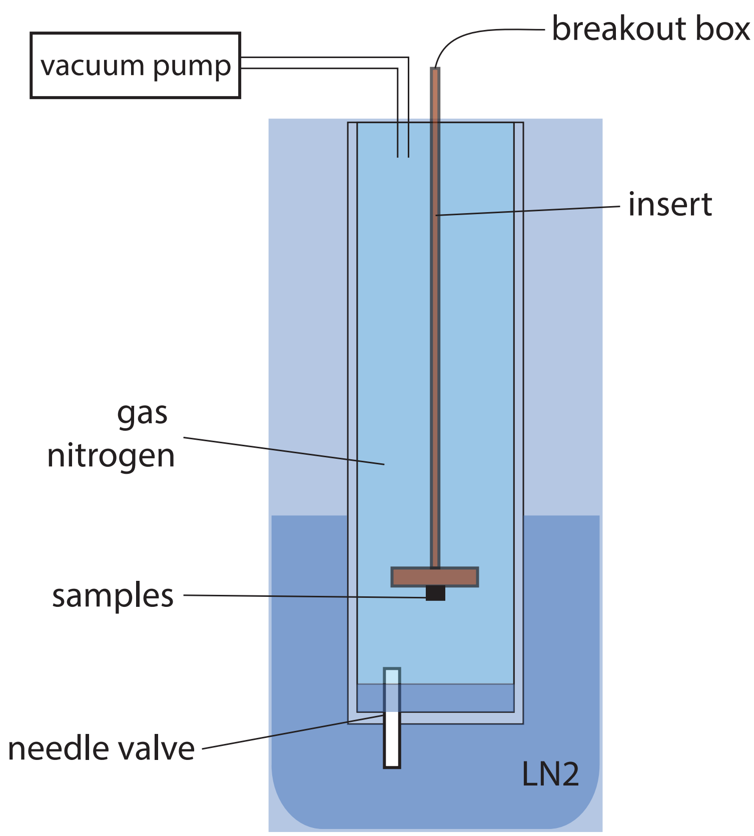

Figure 3.14: Schematic drawing of the VTI cryostat. The samples, situated at the base of the insert, are bathing in gas nitrogen. The communication from the samples to the external apparatus (lock-ins, sourcemeters, etc) is established via wiring passing through the insert rod and connected to a breakout box.

3.4.3 Data taking software

Data is acquired using a Python software written by actual and former members of the lab (B. A. Schmidt, P.-F. Duc, with initial contributions by B. Evert). The software communicates simultaneously with all connected instruments via a GPIB interface. The execution of an experiment requires the creation of a Python script, according to which the software sends instructions and reads from the desired instruments. For instance, a typical conductance pinch-off measurement requires reading voltage from a lock-in amplifier while sweeping (negative) voltage through a Keithley.

Chapter 4

Results

When developing a new experimental approach, effective fabrication methods and challenges encountered are results in themselves. This chapter will first present examples of successful measurements, and then address the difficulties encountered throughout the project along the step-by-step improvement of the flip-chip method.

The ultimate goal of this research project was, and remains, to observe interference between the quasiparticles found in the 5/2 state of the fractional quantum Hall effect in order to determine if they show signs of non-abelian exchange properties. The flip-chip method has proven successful in a number preliminary steps and benchmark measurements, indicating that sustained efforts along this road will likely lead to useful and repeatable observations of quantum oscillations. Flip-chip devices therefore have great potential for probing the 5/2 state via interferometry, and further investigations of other sensitive quantum Hall states.

At this point, the principal accomplishment of this project was to observe a characteristic pinch-off and quantized conductance through a flip-chip QPC. This result lead to a first scientific publication [1] in which the flip-chip was presented as a *method* for ultra-high mobility devices with emphasis put on the novelty of the technique. Along with quantized conductance, customary quantum Hall resistance measurements were taken "through" an interferometer in order to verify if the flip-chip architecture affected negatively the properties of the 2DEG. As a further matter, one flip-chip Fabry-Perot interferometer showed signs of field-dependent quantum interference of electrons. The reliability of this observation will however be discussed, since the oscillations could not be retrieved by a sweep of the central gate of the interferometer. A change in the central enclosed area of the interferometer should also, in theory, result in oscillations in the conductance across an interferometer.

Despite great advances in the fabrication method and a proof that the flip-chip method can reproduce landmark low-dimensional conductance measurements, the nanofabrication yield remains low. Even if the method offers the possibility to reuse samples, the number of working devices is limited by the difficulty to produce absolutely flat surfaces and ensure that the interferometers are in contact equally everywhere. The issue of flatness will be discussed in time, and improvements will be proposed in light of recently published efforts from an independent research group also working on flip-chip devices [19].

4.1 1D conductance quantization

4.1.1 Conventional versus flip-chip QPCs

Conductance pinch-off and quantization can be routinely achieved on moderate mobility AlGaAs/GaAs 2DEG samples (from Sandia National Laboratories, $\sim 2 \times 10^6$ cm^2/Vs). Furthermore, working interferometers and QPCs can usually be conserved and tested again, thus fulfilling one of the project's original goals. Indeed, most flip-chip devices show good resilience to successive cooldown and warm-up cycles, and can be reused and remounted at will. Importantly, within a single cooldown, the gate voltage can be varied without causing significant hysteresis. The absence of hysteresis indicates that charges accumulated in the gates are properly evacuated from the devices. This behavior will be required later to tune the interferometer in a reliable manner.

To observe conductance quantization, the devices are cooled to ∼25 mK in our *Janis* dilution refrigerator and measured via four-point probe low-noise techniques. An example of successful measurement is shown in Figure 4.1, on which quantization of conductance in a flip-chip QPC is compared to that of a conventional integrated QPC [1].

One can notice that the flip-chip QPC reproduces the same plateaus as the con-

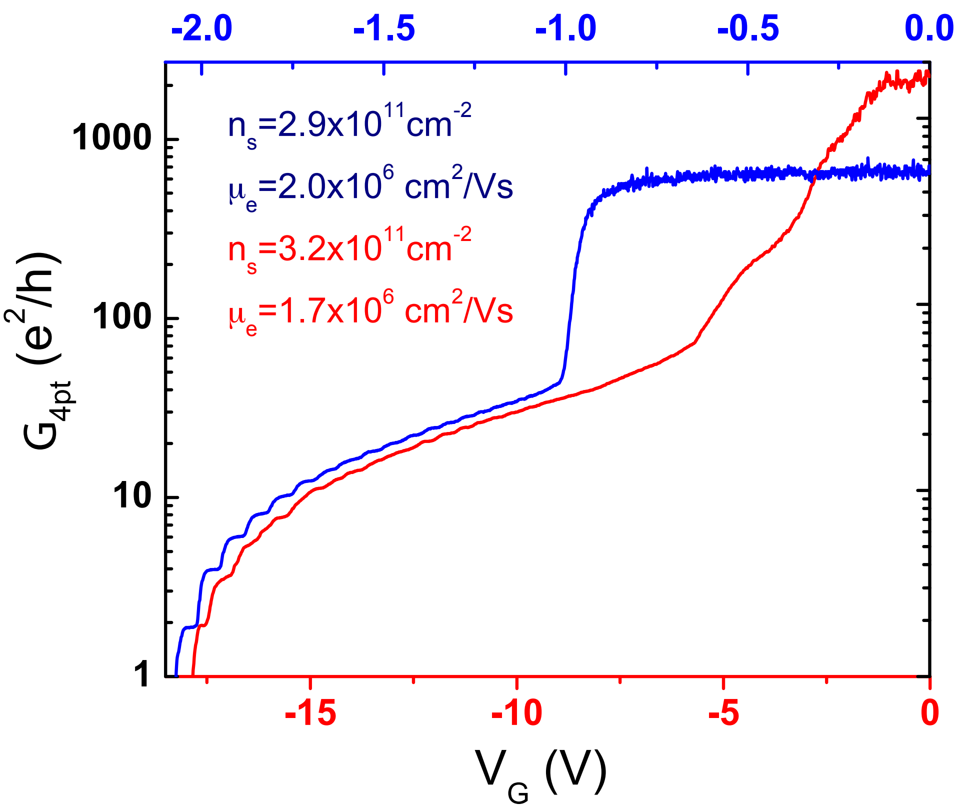

Figure 4.1: Log-scale quantized conductance across a conventional QPC (blue) and flip-chip QPC (red) at 25 mK. The plateaus coincide at even multiples of e^2/h, as expected. Electronic density and mobility are indicated for each 2DEG samples used in this measurement [1].

ventional QPC, although at a much higher pinch-off gating voltage. In the flip-chip case, the QPC pinches off completely just before -13 V, compared to about -2 V for the conventional QPC. Also, the flip-chip QPC plateaus are visibly not defined as well as in the conventional QPC. The observations of "blurred" plateaus at higher gating voltages is attributed to the disposition the devices when mounted in flip-chip, where the distance between the metal gates and 2DEG is globally increased and plausibly non-uniform. Indeed, conventional gates deposited directly on top of the heterostructure are typically separated by about 50 nm (quantum well depth) from the underlying mobile electrons. The metal is evaporated everywhere evenly hence there is no flatness issues, as the gates are in contact with the heterostructure over the whole surface of the devices. In the flip-chip case, the QPCs are necessarily further away due to the application of an insulating ALD coating ($\sim$20-80 nm). It is also difficult to get the flip-chip flat over the whole contact area. The presence of air (vacuum) gaps between the ALD and the heterostructure [1] adds more distance between the gates and the 2DEG, which necessarily augments the voltage required to deplete it.

4.1.2 Ultra-high mobility pinch-off

Being able to reproduce QPC conductance quantization using the flip-chip method is a first step towards the measurement of quasiparticles interference in the fractional quantum Hall regime. However, to reach that goal, it is primordial to be capable of transposing these measurements onto ultra-high mobility 2DEG samples (in excess of 35×10^6 cm^2/Vs). It turns out that working with such samples is trickier than working with moderate mobility ones.

The elaboration of ultra-high mobility samples is complex, contains a large number of steps and require intensive monitoring. The samples are in some sense “handcrafted”. Although the growth technique yields 2DEGs of exceptional quality and mobility, it introduces many known complications. During molecular beam epitaxy (MBE), the wafers do not grow in a perfectly flat manner. The resulting electron density and mobility is thus not uniform: a sample cut from the center of a wafer can have exceptional properties, while another taken further away has risks of not being as good. The flip-chip method solves this problem, but creates another one. Indeed, the reusable flip-chips can always be remounted at a slightly different location on a same sample, which gives the possibility to “browse” for a sweet spot in the 2DEG. With that said, the flip-chip requires absolute surface flatness in order to work optimally. Even a slight warp can prevent the gates from conforming to the surface of the heterostructure over the whole contact area. This issue is a possible explanation for why it has been consistently harder to even simply pinch-off conductance across most ultra-high mobility 2DEG samples. In the conventional fabrication technique, flatness was not a problem since the evaporated metal will always conform to the surface of the substrate, no matter how irregular it is.

Despite the previously mentioned difficulties, it has been possible to use the flip-chip

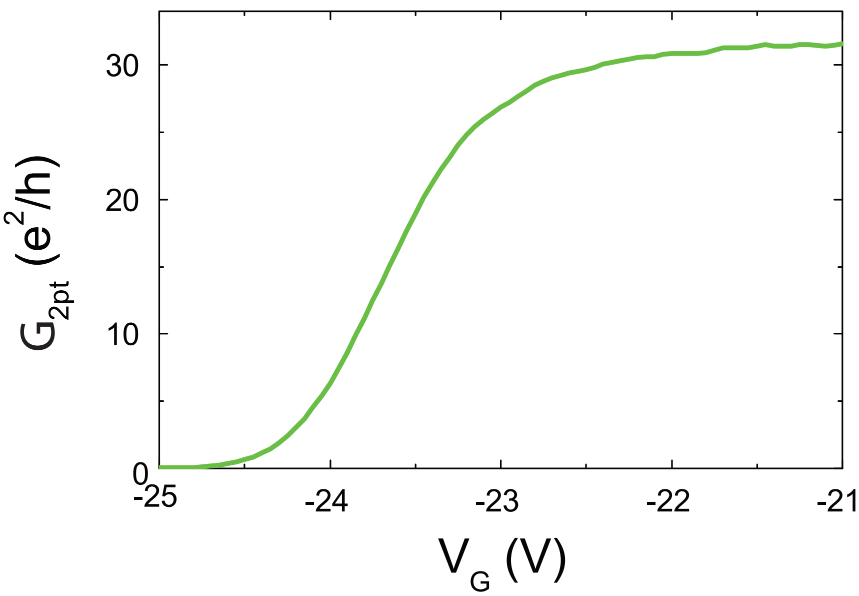

Figure 4.2: Two-point measurement of conductance pinch-off through a flip-chip QPC measured at 4 K on a ultra-high mobility 2DEG ($\sim 1.0 \times 10^7 \text{cm}^2/V \cdot s$) from L. N. Pfeiffer [1].

method on our ultra-high mobility samples. Figure 4.2 shows an example of conductance pinch-off achieved on a ultra-high mobility 2DEG. A large distance between the electrostatic gates and 2DEG explains the particularly high pinch off voltage between -24 and -25 V. Conductance plateaus of $2e^2/h$ are not present here since the 2DEG is at liquid helium temperature (4 K), which is too warm. At sufficiently low temperatures, no flip-chip devices (ordinary QPCs or interferometers) mounted on ultra-high mobility 2DEG samples could reproduce a quantization of conductance as shown in Figure 4.1.

4.2 Hall resistance in a flip-chip

In order to verify the robustness of flip-chip interferometers, and to see if they had an effect on the quality of the 2DEG samples, they were also tested in the quantum Hall regime. The devices themselves have been shown to withstand temperatures of 25 mK and magnetic fields up to 9 T without being damaged. Furthermore, resistance measurements done in various configurations indicated that the main quantum Hall features were preserved in the 2DEG in the presence of an overlaying flip-chip interferometer.

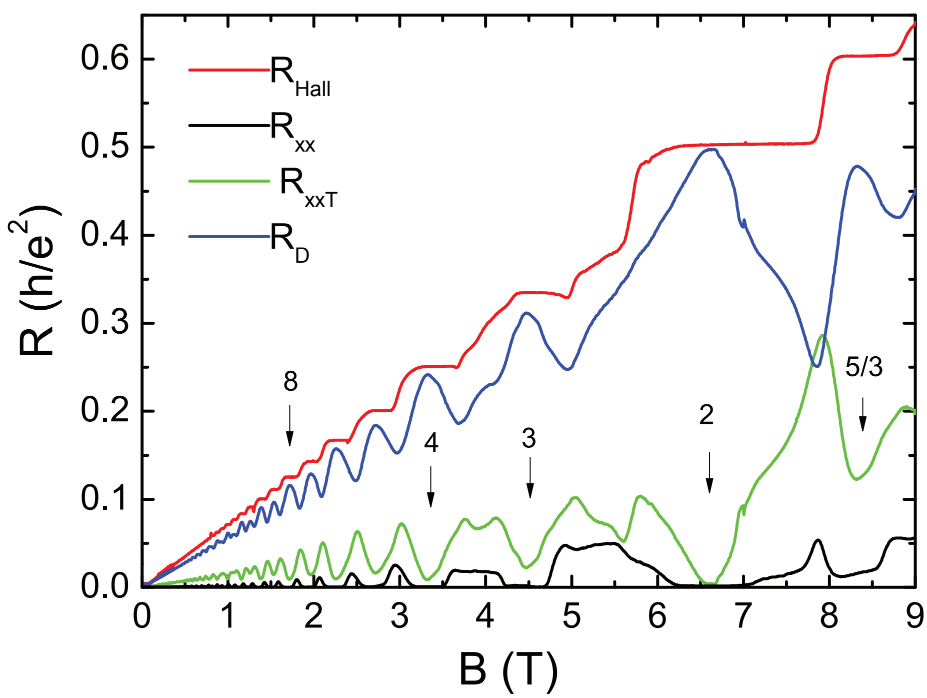

Figure 4.3: Hall resistance (R_{Hall}, red), diagonal resistance (R_D, blue), longitudinal resistance *outside* (R_{xx}, black) and *through* the interferometer (R_{xxT}, green) versus transverse magnetic field in a 2DEG sample from Sandia. Obvious integer and fractional (5/3) quantum Hall hallmarks are present through the pinched QPCs, a feature that is essential for interferometry experiments.

Figure 4.3 shows resistances taken in the quantum Hall regime in different configurations, using a moderate mobility 2DEG (Sandia). R_{Hall} (red) was necessarily taken outside the interferometer with all gates grounded (the disposition of the interferometer, perpendicular to the current flow, does not give access directly to R_{Hall}). The expected quantization of IQH plateaus is noticeable, as well as the 5/3 plateau, expected for 2DEGs of comparable mobility. However, R_D (blue), which is a combination of R_{Hall} and R_{xx}, provides information about the Hall resistance under the interferometer. Despite a large longitudinal contribution, it is still possible to observe the resistance maxima arising at the center of the normal R_{Hall} plateaus. Then, two versions of longitudinal resistance were looked at: R_{xx} (black) taken *under* the interferometer gates, and R_{xxT} (green) taken *through* the interferometer while the QPCs were pinching the 2DEG. The small magnitude of R_{xx} is caused by the relative proximity of the contacts used to test this geometry. The contacts being closer result in a smaller voltage drop, hence the lower resistance. Finally, the usual characteristics are preserved in R_{xxT}, with (almost completely) vanishing longitudinal resistance at allowed filling values. In sum, the method preserves the quality of the 2DEG samples, which confirms another expectation of the flip-chip project.

4.3 Quantum oscillations

Apparent quantum oscillations were observed while testing a Sandia (moderate mobility) flip-chip interferometer. While the QPCs are partially pinching the 2DEG, they enter a regime where they act like beam splitters for electrons. In the IQHE, the electrons circulating in edge currents are then either reflected or transmitted, resulting in interference and diagonal conductance oscillations as the B field is changed (see chapter 1). The field-dependent oscillations that were obtained with our flip-chip interferometers are not very well defined. However, when extracting an average oscillation period ΔB of ≈ 0.018T, using equation 1.28 reveals that the effective central loop area S is be about 450×450 nm^2, which is not unreasonable considering the design of our interferometer. The plausible interference of electrons in the integer quantum Hall regime is presented in Figure 4.4.

An additional element which makes those oscillations ambiguous is that they could not be reproduced by sweeping the central gate voltage. Theory predicts that pinching the central gate will decrease the size of S, resulting in a change of accumulated phase between the transmitted and reflected electrons (analogous to sweeping the B field and changing the flux through S). Such behavior could not be produced, which raises questions concerning the first obtained oscillation results. A deeper investigation will have to be undertaken to determine if our flip-chip method is currently suitable for observation of electron and quasiparticle interference.

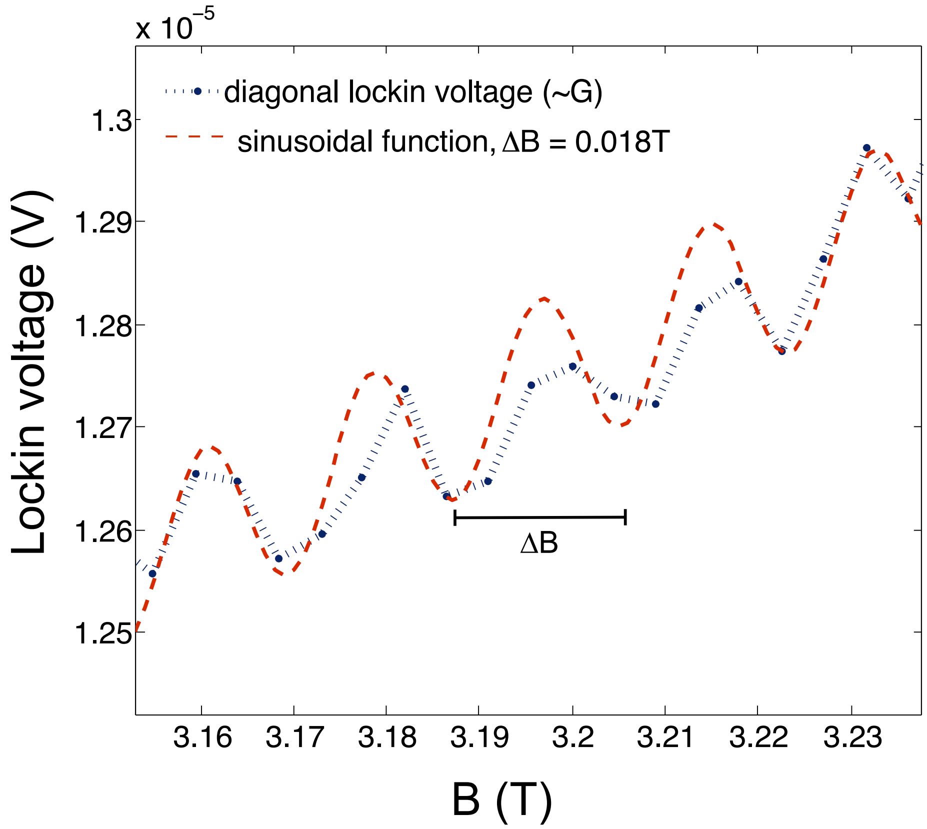

Figure 4.4: Possible field dependent diagonal conductance ($\propto$ lockin voltage) oscillations due to interference of electrons in the integer quantum Hall regime. The dimensions of the central box of the Fabry-Perot interferometer is $2 \times 1.5 = 3\mu\mathrm{m}^2$. Extracting the period ΔB and making use of equation 1.28 yields an effective central loop of area $S \approx 0.2\mu\mathrm{m}^2$, a result consistent with electron interference.

4.4 Main issues

The principal fabrication challenge is to ensure the flatness of the two surfaces of the flip-chip (2DEG and interferometer). In spite of all taken precautions (cleanroom processing, cleaning, etc), it is difficult to make sure that there is *absolutely* no dusts on the 2DEG *and* on the interferometer. Recall that the thickness of the metal layer of the interferometers is about 150nm. Any contamination from a dust particle with dimensions larger than that could tilt the flip-chip and thereby introduce an air gap (vacuum) between two surfaces. Such a gap increases drastically the gate voltage required to pinch-off the 2DEG due to the dielectric constants of air, possibly trapped water vapor and helium/nitrogen gas, which makes it hard to have all three interferometer QPCs working correctly. The flatness issue could be improved by reducing the contact area between the surfaces that are mechanically held in contact [1]. Solutions such as creating large pillars lifting slightly but evenly the interferometer, or etching the heterostructure to reduce the contact area, were tried and shown successful by Kouwenhoven's research group working on similar flip-chip devices [19].

Next, current leaks were found to be regular source of struggle when testing the flip-chip devices. Our solution was to apply an insulating ALD (Al_2O_3) of about 30 to 100nm to enclose the interferometers, thus preventing charges from escaping the electrostatic gates. However, the mobile electrons of Pfeiffer's ultra-high mobility 2DEGs are already situated at a few tens of nanometers below the sample's surface (various depths depending on the sample). Adding ALD increases significantly the distance between the gates and the gas, which once again increases the voltage required to deplete it. We often observed that the conductance pinch-off never occurred, even at gating voltage as high a -60V. In comparison, some samples on Sandia 2DEGs could be totally pinched before reaching -10V. As reported by Willett [36], one of the challenges in the study of the 5/2 state is that the ultra-high mobility wafers *must* be designed such that the 2DEG is deeper below the surface. This is part of the reasons why flip-chips mounted on Sandia wafers are easier to use. In sum, while preventing leaks, our approach also brings the interferometers very far away from the 2DEG, requiring extremely high gating voltages. This situation could be avoided by leaving out ALD and engineering the flip-chips such as to purposefully leave a small air gap between the interferometers and heterostructures. Again, this strategy was recently employed by Kouwenhoven to conduct successful flip-chip interferometry measurements [19].

Chapter 5

Conclusion

5.1 Closing remarks

The ultimate objective of the flip-chip anyon interferometer project was to observe interference of quasiparticles in the 5/2 state of the fractional quantum Hall effect. In two dimensions, the exchange properties of particles are not limited to fermionic or bosonic behaviors. Instead, changing the topology of the configuration space opens up a continuous range of *anyonic* statistical phases governed by *braiding* operations, ranging between Fermi-Dirac and Bose-Einstein exchange statistics. Anyons are now well understood within the composite fermions picture of the fractional quantum Hall effect, and consist of electrons bound to flux quanta in a ratio described by the filling factor ν. The 5/2 state, however, remains a mystery because of its even denominator, and stands as the exception to the composite fermion rule governing allowed ν values. Among the models proposed to explain the seemingly incompatible nature of the state, the Moore-Read Pfaffian attracted attention among the community since it described the 5/2 quasiparticles as Majorana bound states with non-abelian exchange properties.

In order to probe the statistics of the 5/2 states, a promising approach is to attempt interferometry manipulations through which quasiparticles are braided one around another. Interferometry experiments were used to demonstrate the existence of anyons and fractional statistics in the FQHE. Yet, it appears that transposing these experiments in the 5/2 state is a harder task due to its extreme fragility, making it observable only in the highest mobility 2DEG samples. Furthermore, it is suspected that some nanofabrication steps performed directly on the 2DEG, notably e-beam lithography, can tarnish irreparably its quality and make strong 5/2 features very difficult to observe. In order to tackle the fragility of the 5/2 state, this research project proposed to implement a flip-chip Fabry-Perot interferometer. In this method, the interferometers are fabricated independently on a sapphire substrate, and then flipped against the heterostructure as if the devices had initially been patterned on it. The hope was that the method would leave the 2DEG in pristine conditions, thus allowing to probe robust 5/2 states via interferometry.

Interferometers were successfully fabricated by e-beam lithography on sapphire substrates. Mounted in flip-chip configuration, those interferometers were tested on moderate and ultra-high mobility 2DEG samples. The expected QPC quantization of conductance could be observed through samples of moderate mobility, with efficiency comparable to QPCs fabricated by conventional metal evaporation methods. It was also possible to pinch-off the conductance of an ultra-high mobility 2DEG, although further investigations must be done in order to understand why it is harder to operate flip-chips on these samples. Still, the flip-chip devices did not seem to affect the quality of the underlying 2DEG, as demonstrated by quantum Hall resistance measurements in different configurations. This result indicates that the flip-chip fulfills one of its main goal, that is: to preserve the 2DEG mobility by avoiding damaging processing steps. Furthermore, flip-chip devices were resilient to multiple cooldown cycles and could effectively be reused and remounted on different samples. This facilitates sample testing, increases the fabrication yield and allows to preserve the precious 2DEG materials.

The flip-chip method has however one main drawback: the flatness of the devices and samples becomes absolutely crucial. Indeed, conventional metal deposition methods will conform to any surface. This flip-chip requires joining and holding mechanically two separate pieces and obtain a device that should be equivalent. This is difficult mainly due to the imperfection of the ultra-high mobility 2DEG samples, chemical contamination and dust particles. Solutions for the flatness issue are currently being elaborated. Those propose to reduce the contact area by etching the heterostructures and leaving only a thin strip on which a small fraction of the interferometers would be touching, or to purposefully create a gap between the devices and the heterostructures by using 'pillars' surrounding the gates (idea implemented by [19]).

In sum, although it has not *yet* been possible to observe anyon interferometry using our flip-chip devices, the method itself seems promising. The possibility to reuse devices on different samples is particularly suited for further study of the sensitive fractional quantum Hall effect and its 5/2 state, which appears only in the highest quality 2DEG samples.

References

[1] K. Bennaceur, B. A. Schmidt, S. Gaucher, D. Laroche, M. P. Lilly, J. L. Reno, K. W. West, L. N. Pfeiffer, and G. Gervais. Mechanical Flip-Chip for Ultra-High Electron Mobility Devices. *Scientific Reports*, 5(13494), September 2015.

[2] Frank Wilczek. Quantum Mechanics of Fractional-Spin Particles. *Physical Review Letters*, 49(14):957–959, Octobe 1982.

[3] J. K. Jain. Composite-fermion approach for the fractional quantum Hall effect. *Physical Review Letters*, 63(2):199–202, July 1989.

[4] R. Willett, J. P. Eisenstein, H. L. Störmer, D. C. Tsui, A. C. Gossard, and J. H. English. Observation of an even-denominator quantum number in the fractional quantum Hall effect. *Physical Review Letters*, 59(15):1776–1779, October 1987.

[5] N. Read and G. Moore. Fractional Quantum Hall effect and Nonabelian Statistics. *Progress of Theoretical Physics Supplements*, 107:157–166, Januray 1992.

[6] Michael H. Freedman, Alexei Kitaev, Michael J. Larsen, and Zhenghan Wang. Topological quantum computation. *Bull. Amer. Math. Soc.*, 40:31–38, October 2003.

[7] Bernd Rosenow, Bertrand I. Halperin, Steven H. Simon, Bernd Rosenow, Bertrand I. Halperin, Steven H. Simon, and Ady Stern. Exact Solution for Bulk-Edge Coupling in the Non-Abelian $\nu = 5/2$ Quantum Hall Interferometer. *arXiv*, page 12, June 2009.

[8] C. de C. Chamon, D. E. Freed, S. A. Kivelson, S. L. Sondhi, and X. G. Wen. Two point-contact interferometer for quantum Hall systems. *Phys. Rev. B*, 55(4), January 1997.

[9] A. Stern and B. I. Halperin. Proposed experiments to prove the $\nu = 5/2$ quantum Hall state. *Physical Review Letters*, 96:016802, January 2006.

[10] Parsa Bonderson, Alexei Kitaev, and Kirill Shtengel. Detecting Non-Abelian Statistics in the $\nu = 5/2$ Fractional Quantum Hall State. *Phys. Rev. Lett.*, 96(1):016803, Januray 2006.

[11] Roni Ilan, Eytan Grosfeld, and Ady Stern. Coulomb Blockade as a Probe for Non-Abelian Statistics in Read-Rezayi States. *Phys. Rev. Lett.*, 100(8):086803, February 2008.

[12] Bertrand Halperin, Ady Stern, Izhar Neder, and Bernd Rosenow. Theory of the Fabry-Pérot quantum Hall interferometer. *Physical Review B*, 83(15):1–17, April 2011.

[13] F. E. Camino, Wei Zhou, and V. J. Goldman. Aharonov-Bohm Superperiod in a Laughlin Quasiparticle Interferometer. *Phys. Rev. Lett.*, 95(4):246802, December 2005.

[14] V. J. Goldman, F. E. Camino, and Wei Zhou. Realization of a Laughlin Quasiparticle Interferometer: Observation of Anyonic Statistics. *AIP Conference Proceedings*, 850(1):1341–1342, 2006.

[15] Wei Zhou, F. E. Camino, and V. J. Goldman. Quantum Transport in an Aharonov-Bohm Electron Interferometer. *AIP Conference Proceedings*, 850(1):1351–1352, 2006.

[16] Nissim Ofek, Aveek Bid, Moty Heiblum, Ady Stern, Vladimir Umansky, and Diana Mahalu. Role of interactions in an electronic Fabry–Perot interferometer operating in the quantum Hall effect regime. *Proc. Natl. Acad. Sci.*, 107(12):5276–5281, February 2010.

[17] R. L. Willett, L. N. Pfeiffer, and W. West. Measurement of filling factor 5/2 quasiparticle interference with observation of charge e/4 and e/2 period oscillations. *Proc. Natl. Acad. Sci.*, 106(22):8853–8858, March 2009.

[18] R. L. Willett, L. N. Pfeiffer, and K. W. West. Alternation and interchange of e/4 and e/2 period interference oscillations consistent with filling factor 5/2 non-Abelian quasiparticles. *Phys. Rev. B*, 82(20):205301, November 2010.

[19] Arjan J. A. Beukman, Fanming Qu, Ken W. West, Loren N. Pfeiffer, and Leo P. Kouwenhoven. A Noninvasive Method for Nanoscale Electrostatic Gating of Pristine Materials. *Nano Letters*, 15(10):6883–6888, September 2015.

[20] Avinash Khare. *Fractional Statistics and Quantum Theory.* World Scientific, 2^{nd} edition, 2005.

[21] G. S. Canright and S. M. Girvin. Fractional Statistics: Quantum Possibilities in Two Dimensions. *Science*, 247(4947):1197–1205, March 1990.

[22] Parsa Hassan Bonderson. *Non-Abelian Anyons and Interferometry.* PhD thesis, California Institute of Technology, 1200 East California Boulevard, Pasadena, May 2007.

[23] BJ Van Wees, H Van Houten, CWJ Beenakker, JG Williamson, LP Kouwenhoven, D Van der Marel, , and CT Foxon. Quantized Conductance of Point Contacts in a Two-Dimensional Electron Gas. *Physical Review Letters*, 60(9):848–850, February 1988.

[24] D. A. Wharam, T. J. Thornton, R. Newbury, M. Pepper, H. Ahmed, J. E. F. Frost, D. G. Hasko, D. C. Peacock, D. A. Ritchie, and G. A. C. Jones. One-dimensional transport and the quantisation of the ballistic resistance. *J. Phys. C: Solid State Phys*, 21(8):L209–L214, March 1988.

[25] Shuichi Murakami. Two-dimensional topological insulators and their edge states. *Journal of Physics: Conference Series*, 302(1), 2011.

[26] Cory Dean. *A Study of the Fractional Quantum Hall Energy Gap at Half Filling.* PhD thesis, McGill University, 845 Sherbrooke Street West, Montreal, Novermber 2008.

[27] K. v. Klitzing, G. Dorda, and M. Pepper. New Method for High-Accuracy Determination of the Fine-Structure Constant Based on Quantized Hall Resistance. *Physical Review Letters*, 45(6):494–497, August 1980.

[28] R. B. Laughlin. Quantized Hall conductivity in two dimensions. *Physical Review B*, 23(10):5632–5633, May 1981.

[29] Douglas T. McClure. *Interferometer-Based Studies of Quantum Hall Phenomena.* PhD thesis, Harvard University, 2012.

[30] D. C. Tsui, H. L. Stormer, and A. C. Gossard. Two-Dimensional Magnetotransport in the Extreme Quantum Limit. *Physical Review Letters*, 48(22):1559–1562, May 1982.

[31] A. Stern. Anyons and the quantum Hall effect - A pedagogical review. *Annals of Physics*, 323:204–249, November 2007.

[32] R. B. Laughlin. Anomalous Quantum Hall Effect: An Incompressible Quantum Fluid with Fractionally Charged Excitations. *Physical Review Letters*, 50(18):1395–1398, May 1983.

[33] F. D. M. Haldane. Fractional Quantization of the Hall Effect: A Hierarchy of Incompressible Quantum Fluid States. *Physical Review Letters*, 51(7):605–608, August 1983.

[34] B. I. Halperin. Statistics of Quasiparticles and the Hierarchy of Fractional Quantized Hall States. *Physical Review Letters*, 52(18):1583–1586, April 1984.

[35] B. I. Halperin. Theory of the quantized Hall conductance. *Helv. Phys. Acta*, 56:75–102, 1983.

[36] R. L. Willett. The quantum Hall effect at 5/2 filling factor. *Reports on Progress in Physics*, 76(7), July 2013.

[37] F. D. M. Haldane and E. H. Rezayi. Spin-singlet wave function for the half-integral quantum Hall effect. *Physical Review Letters*, 60(10):956–959, March 1988.

[38] A. Yu. Kitaev. Fault-tolerant quantum computation by anyons. *Annals of Physics*, 303(1):2–30, January 2003.

[39] Hyunjin Lee et al. Sub-5nm All-Around Gate FinFET for Ultimate Scaling. In *VLSI Technology, 2006. Digest of Technical Papers. 2006 Symposium on*, pages 58–59, 2006.

[40] Bram Evert. Electrical Transport, Filtering and NMR of GaAs/AlGaAs Quantum Wires. Master's thesis, McGill University, November 2013.